NASA CONTRACTOR REPORT

NASA CR-61368

PREPARATION AND EVALUATION OF APOLLO 14 COMPOSITE EXPERIMENTS

By W. H. Steurer and S. Kaye
Convair Aerospace Division of
General Dynamics
P.O. Box 1128
San Diego, California 92112

August 1971

Prepared for

NASA-GEORGE C. MARSHALL SPACE FLIGHT CENTER
Marshall Space Flight Center, Alabama 35812

TECHNICAL REPORT STANDARD TITLE PAGE

1. REPORT NO. NASA CR-61368	2. GOVERNMENT ACCESSION NO.	3. RECIPIENT'S CATALOG NO.
4. TITLE AND SUBTITLE PREPARATION AND EVALUATION OF APOLLO 14 COMPOSITE EXPERIMENTS		5. REPORT DATE August 1971 6. PERFORMING ORGANIZATION CODE
7. AUTHOR (S) W. H. Steurer and S. Kaye		8. PERFORMING ORGANIZATION REPORT # GDCA-DBG71-009
9. PERFORMING ORGANIZATION NAME AND ADDRESS Convair Aerospace Division of General Dynamics P.O. Box 1128 San Diego, California 92112		10. WORK UNIT NO. 11. CONTRACT OR GRANT NO. NAS 8-24979
12. SPONSORING AGENCY NAME AND ADDRESS National Aeronautics and Space Administration Washington, D. C. 20546		13. TYPE OF REPORT & PERIOD COVERED Contractor Report 14. SPONSORING AGENCY CODE

15. SUPPLEMENTARY NOTES

Technical Monitor: Iva C. Yates, PT Laboratory, George C. Marshall Space Flight Center

16. ABSTRACT

The objective of the basic contract, NAS8-24979, Processes for Space Manufacturing, was an evaluation of all potential processes, the definition of the most effective processing concepts and products, and the establishment of developmental programs as indicated by the identified process requirements. It included a detailed assessment of all pertinent fundamentals, many of which had to be adapted to the peculiar requirements of processing under zero-g since there was no precedent. The final report containing details on all outlined subjects was submitted to MSFC in June 1970 (Report GDC-DBG-70-001).

The present report gives an account of the work performed in an extension of the basic contract aimed at flight experiments on Apollo 14. The objectives of this work were: (1) evaluation and selection of suitable materials, (2) definition of in-flight processing procedures, (3) preparation of pre-processed materials and delivery to MSFC, and (4) evaluation of the space-processed samples after return from the Apollo 14 flight.

Most of the work related to the sample preparation (1, 2, 3 above) was carried out in the form of laboratory investigations and experiments since the severe time limitations did not permit detailed theoretical studies. The experimental development of the in-flight mixing procedure was documented in a motion picture, submitted to MSFC-S&E-PT in December 1970.

17. KEY WORDS	18. DISTRIBUTION STATEMENT Iva C. Yates, Jr. Unclassified-unlimited

19. SECURITY CLASSIF. (of this report)	20. SECURITY CLASSIF. (of this page)	21. NO. OF PAGES	22. PRICE
U	U	70	$3.00

MSFC - Form 3292 (May 1969)

FOREWORD

This report summarizes the work carried out by the Convair Aerospace Division of General Dynamics in connection with the Apollo 14 demonstration experiments and under Contract NAS 8-24979 for the Product Engineering and Process Technology Laboratory, Marshall Space Flight Center. The program was administered and monitored by I. C. Yates, Jr. (S&E-PT-A), supported by E. C. McKannan (S&E-ASGN-MM). Basic guidelines and objectives were established by H. F. Wuenscher, Assistant Director for Advanced Projects (S&E-PT-DIR).

The work was carried out by the space manufacturing team of Convair Aerospace, under the direction of Dr. W. H. Steurer and D. J. Gorham, who served as program coordinator. Materials investigations and evaluations were conducted by Dr. S. Kaye, with the assistance of J. Pardubsky and T. Hursman in the field of laboratory experimentation, and Dr. M. Miller in metallurgical evaluations. Flight processing experiments were carried out by G. B. Wood.

TABLE OF CONTENTS

TABLE OF CONTENTS, Contd

INTRODUCTION

The objective of the basic contract, NAS8-24979, Processes for Space Manufacturing, was an evaluation of all potential processes, the definition of the most effective processing concepts and products, and the establishment of developmental programs as indicated by the identified process requirements. It included a detailed assessment of all pertinent fundamentals, many of which had to be adapted to the peculiar requirements of processing under zero-g since there was no precedent. The final report containing details on all outlined subjects was submitted to MSFC in June 1970 (Report GDC-DBG-70-001).

The present report gives an account of the work performed in an extension of the basic contract aimed at flight experiments on Apollo 14. The objectives of this work were: (1) evaluation and selection of suitable materials, (2) definition of in-flight processing procedures, (3) preparation of pre-processed materials and delivery to MSFC, and (4) evaluation of the space-processed samples after return from the Apollo 14 flight.

Most of the work related to the sample preparation (1, 2, 3 above) was carried out in the form of laboratory investigations and experiments since the severe time limitations did not permit detailed theoretical studies. The experimental development of the in-flight mixing procedure was documented in a motion picture, submitted to MSFC-S&E-PT in December 1970.

The following report is divided into seven major sections:

1. Evaluation of Matrix Materials
2. Evaluation of Reinforcement Materials
3. Composite Experiments
4. Selection of Experiment Materials
5. Preparation of Materials for Flight Samples
6. Development of Mixing Techniques
7. Evaluation of Samples 5 and 11

During the time of materials evaluation and experiment preparation, close communication was maintained with the contract monitor and numerous technical decisions were made by telephone discussion of laboratory experiment results. For this reason, laboratory evaluations that are not significant for future work have been omitted from this report. Likewise omitted is the preparation of the flight and control specimen (filling of experiment capsules) as it was carried out by MSFC-S&E-PT.

SECTION 1
EVALUATION OF MATRIX MATERIALS

The planned Apollo 14 experiments called for the definition of two types of base (matrix) materials: (1) a metal or alloy and (2) a transparent or, at least, translucent material - both with a melting temperature between 105 and 170°F (40 and 76°C).

1.1 MATRIX METAL SELECTION

The selection of the matrix material was limited by experiment constraints to a maximum melting temperature of 170°F. Attention was focused on Bi-base alloys with various combination of Pb, Sn, Cd, and In which exhibit a number of eutectics with melting temperatures between 110 and 170°F. Preliminary casting experiments were carried out with the following alloys:

Trade Name	Constituents	Melting Temp.
Cerrolow 117	Bi, Pb, In, Sn, Cd	117°F
Cerrolow 136	Bi, Pb, In, Sn	136°F
Cerrobend	Bi, Pb, Sn, Cd	158°F

Cerrobend was selected for the initial laboratory experiments, for the following reasons:

a. Acceptable melting temperature.

b. Good strength and creep resistance (other alloys creep at room temperature under very low loads).

c. Its density differs by a good margin from all considered reinforcement materials, providing an effective demonstration of the zero-g mixture stability.

While most laboratory work was carried out with this alloy, it was, in view of the toxicity of its Cd content, replaced during the latter part of the program by a eutectic 66 In - 34 Bi alloy. The toxicity of Cd is evaluated quantitatively in Section 1.4. However, most of the data obtained with Cerrobend apply equally to the Bi-In alloy. The nominal properties of the two alloys are:

	Cerrobend		In-Bi	
Composition	Bi	50%	In	66%
	Pb	26.7%	Bi	34%
	Sn	13.3%		
	Cd	10%		
Density	9.35 gm/cm^3		8.555 gm/cm^3	
Melting Temp	158°F		162°F	
Strength *	6000 psi		2000 psi	

* Nominal strength. More accurate data follow.

1.2 MATRIX-METAL STRENGTH

For the determination of the tensile strength of the two base metals, tensile samples with 1/2-inch diameter and 3-inch gage length were cast in a pre-heated aluminum mold. Tests were carried out at room temperature, 0°C, and -78°C. The purpose of the low temperature tests was the consideration that these low-melting alloys are in a similar high plasticity state at room temperature, as are engineering materials at temperatures approaching their melting points. As illustrated in Figure 1-1, a low temperature of the experiment materials represents a condition equivalent to aluminum or steels at room temperature. Less variation of test values is expected at this condition.

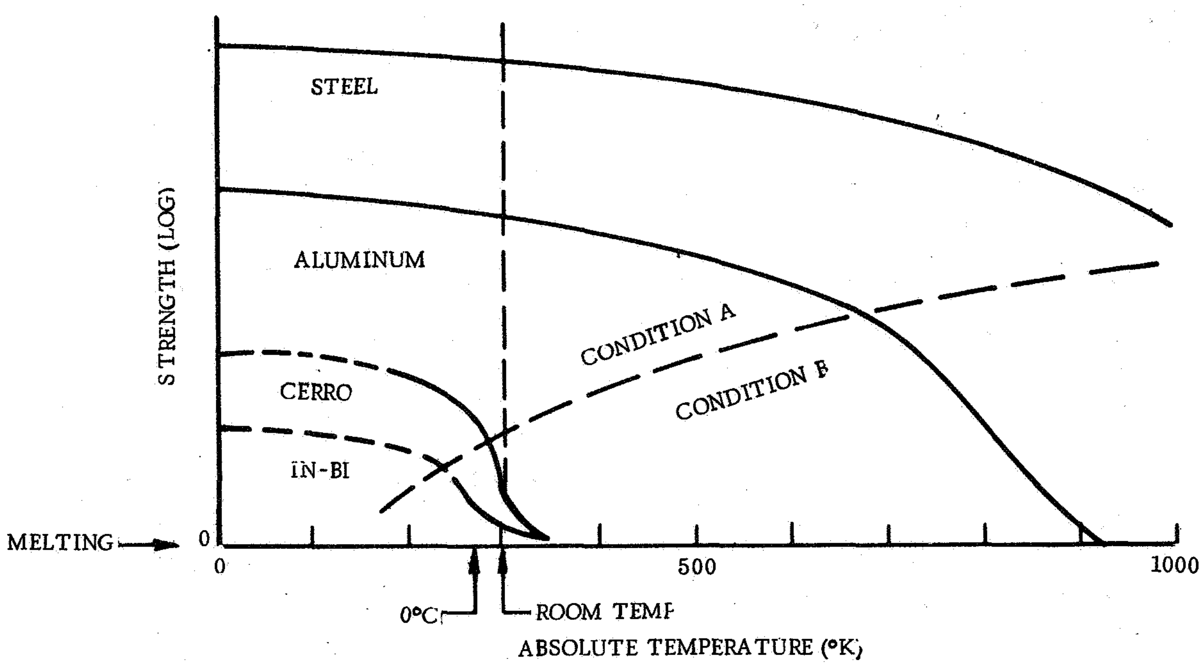

A = HIGH STRENGTH (ELASTIC RUPTURE)
B = STRENGTH DECAY (PLASTIC RUPTURE)

Figure 1-1. Strength of Metals vs. Temperature

The results of the tensile tests of the two base materials are:

Alloy	Test Temp (°C)	UTS (psi)
Cerrobend	24	2407
	0	6012
	-78	7509
In-Bi (66/34)	25	1261
	0	2293

The significant strength increase of Cerrobend between room temperature and 0°C, and the relatively small further increase at -78°C show that this material is, for all practical purposes, in Condition A (Figure 1-1) at 0°C. This temperature was adopted as standard test temperature; it can be easily maintained by enclosing any test fixture in an ice-water-filled plastic bag.

For In-Bi, tests at -78°C could not be carried out due to time limitations. While it shows a substantial strength increase between room temperature and 0°C, it is questionable, in the absence of lower-temperature values, whether it has already reached Condition A at 0°C.

1.3 COLD WORKING CHARACTERISTICS OF CERROBEND

The initial (tentative) experiment program included a metal matrix with fully dispersed oxide particles as a base material for a dispersion-strengthened material with improved creep resistance. In such materials, the strength is obtained by cold working, while the dispersed particles stabilize the so-strengthened microstructure to higher temperatures. It was, therefore, necessary to evaluate the adaptability of Cerrobend to cold working.

Cold working experiments were carried out with 1/2-inch thick slugs in a rolling mill and a press. At room temperature, the material fractured even at low reductions. Good results were obtained at higher temperature (Figure 1-2). The optimum temperature was defined as 52°C which combines a reduction capability of 50% with, at least, some strenghening effect (the degree of recrystallization was not investigated).

1.4 TOXICITY OF CADMIUM

During the course of the program, questions arose concerning the toxicity of cadmium, which was a component of the Cerrobend alloy. A calculation was therefore made about the extent of the hazard arising from the presence of cadmium.

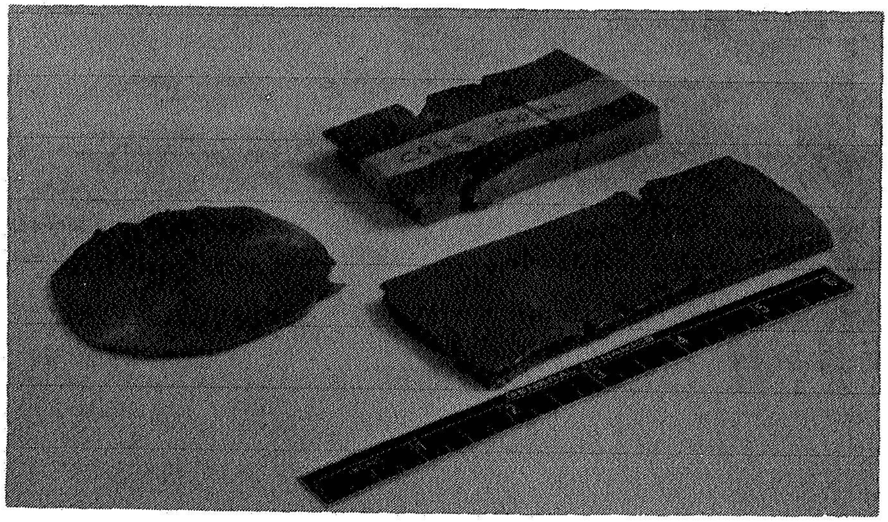

Figure 1-2. Cold Working Experiments With Cerrobend

The official value for the threshold limit value (TLV) of cadmium published by the American Conference of Governmental Industrial Hygienists in 1969 is 0.2 milligram per cubic meter. This exposure is permissible for continuous periods of 8 hours per day for a 5-day week with no adverse effect expected.

The vapor pressure of pure cadmium at 150°C is 9×10^{-5} mm Hg. This is equivalent to 0.1 part per million (ppm) or 0.466 mg per cubic meter as determined by applying the factor 0.02404/mol. wt. The actual content of cadmium in Cerrobend is about 10%, so the actual concentration developed in an atmosphere at equilibrium with the hot alloy would be 0.0466 mg per cubic meter or one-fifth the TLV. The concentration data versus temperature are plotted in Figure 1-3.

This result must be considered in the light of the following facts:

a. The vapor pressures reported above are equilibrium vapor pressures and require a continuous heat source to maintain the concentration.

b. The cadmium is alloyed. The actual ideal vapor pressure corresponds to the mole fraction of cadmium in the alloy or about 10% of the equilibrium vapor pressure for the pure metal.

c. If a capsule breaks, the spilled metal will cool rapidly and condense.

We may conclude, therefore, that the presence of cadmium in Cerrobend presents no toxic hazard if a capsule at 150°C breaks and exposes personnel to the metal vapor. The practical danger at 150°C should not be greater than for In, which has a TLV of 0.1 mg per cubic meter.

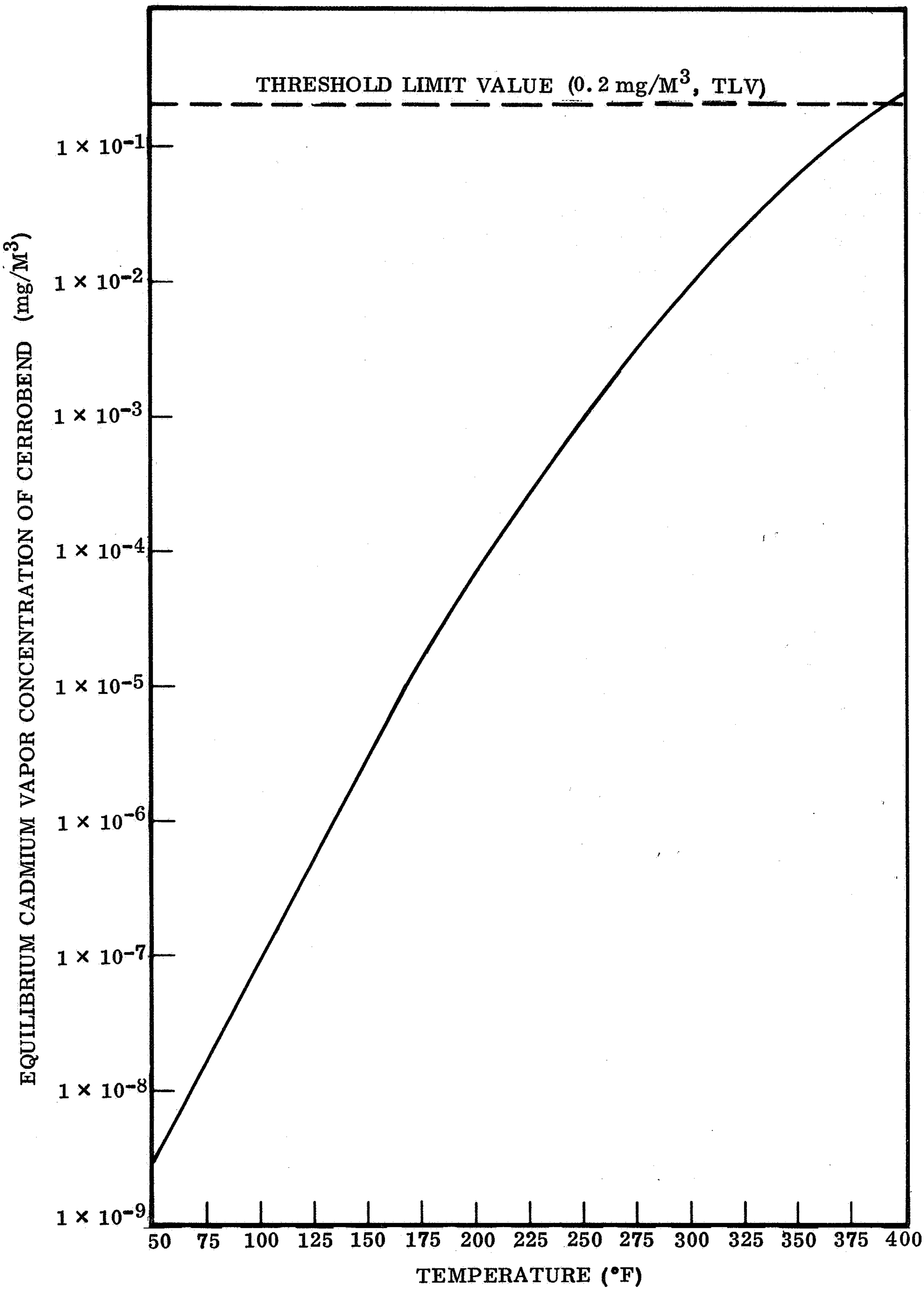

Figure 1-3. Cadmium Vapor Concentration vs. Temperature

1.5 TRANSPARENT MATRIX SELECTION

The planned flight experiments with a transparent matrix had the objectives: (1) to produce a directly-visible demonstration of the zero-g mixture stability and (2) to obtain dispersion control samples for the opaque composites. Numerous compounds, with expected melting points or solid-liquid ranges in the 45°C to 70°C regime, were evaluated in laboratory experiments. The evaluated materials are listed in Table 1-1. All were tested as aqueous solutions at various concentrations, measuring the solid-liquid transition temperature and observing qualitatively the solid-state consistency and the liquid-state transparency. Most of these materials were eliminated for such reasons as lack of transparency, flammability, toxicity, or necessity of catalyst deployment. The most promising base materials were gelatine (protein) and polysaccharides. Both are used in aqueous solutions and absolutely nontoxic (edible). Softening and melting temperature, as well as viscosity and transparency can be controlled over a wide range by concentration.

More extensive experiments were carried out with these two base materials and various additives in attempts to raise the melting temperature and lower the liquefaction temperature. This was done by preparing various combinations of matrix with salts, acids, gums, polymers and protein bases using stock solutions of base material. The general conclusion of the experiments was as follows:

a. Additives have little, if any, effect for achieving the desired properties of both gelatine and polysaccharide. The gelatines and polysaccharides are not compatible with one another.

b. The melting temperature and the consistency below the melting point are primarily determined by concentration.

The relationship between concentration and melting point, liquid state viscosity, gel consistency and transparency was determined experimentally. The results indicated the following optimum concentrations:

Gelatine (Knox)	7%
Plysaccharide (Burtonite 44)	1.5%

During reentry, the Apollo command module interior may reach a temperature of 110°F. Considering the short time of this heat pulse, the maximum sample temperature is expected to remain below 105°F. However, even this temperature rules out gelatine (melting temp 87-90°F). Burtonite is at 105°F sufficiently firm (see Section 1.7) to maintain mixture stability even at the high g-loads encountered during reentry. Burtonite 44 was, therefore, proposed as transparent matrix material.

Table 1-1. Screening Materials for Transparent Matrix

Material	Source
Proteins	
Gelatine	Knox Gelatine Inc., Johnstown, N.Y.
Crystal Gelatine	Eastman Gelatine Corp., Peabody, Mass.
Gen Gel	General Mills Chemicals, Inc., Minneapolis, Minn.
Gum Arabic	Shelf (GGA)*
Casein	Shelf (GGA)
Zein	Shelf (GGA)
Swifts Colloid	Shelf (GGA)
Saccharides and Hydroxy Polymers	
Burtonite 44	Burtonite Co., Nutley, N.J.
Kelgum	Kelco Co., San Diego, Ca.
Starch	Corn Products Refining Co., Argo, Ill.
Apple Pectin	Shelf (GGA)
Agar Agar	Shelf (GGA)
Hydroxyethylmethacrylate Copolymer	Hercules (GGA)
Carboxymethylhexaethyl Cellulose	Shelf (GGA)
Hydroxypropyl Cellulose and other Derivatives	Hercules Inc., Los Angeles, Ca.
Organic Acids and Hydrocarbons	
Glycerin Soap	Colonia Inc., Distributors, New York, N.Y.
Neutrogena Soap	Neutrogena, Los Angeles, Ca.
Transparent Soap	A&F Pears Ltd., London, England
Paraffin	American Oil Co., Chicago, Ill.
Polymers	
Polyvinyl Alcohol	Shelf (GGA)
Polyvinylpyrrolidone	General Aniline and Film
Acrysol	Rohm and Haas, Philadelphia, Pa.
Polymers F-3, 705 D-B, 1212A, SB, Jaguar Plus	Stein, Hall & Co., Inc., New York, N. Y.
Inorganics	
Sodium Silicate	Shelf (GGA)

* Gulf-General Atomic, San Diego, California

The only drawback of these aqueous solutions, including Burtonite, is the danger of boiling and the associated pressure increase if the cartridge temperature exceeds 212°F during the flight experiment. In the final transparent material selection, therefore, Burtonite was replaced by paraffin. Even though paraffin is merely translucent after solidification, it has a safe boiling temperature. Consequently, the direct-visibility demonstration had to be abandoned in favor of laboratory evaluation of a translucent composite. However, in view of its solid-state transparency, Burtonite 44 may be considered for a later flight experiment with more accurate temperature control. Therefore, the properties are listed together with those of paraffin:

	Burtonite 44	Paraffin
Concentration, %	1.5	(Am. Oil Co.)
Density	1.0	0.872
Melting Temperature, °F	115	133
Boiling Temperature (1 atm.), °F	212	581
Light Transmission		
Solid	Transparent	Translucent
Liquid	Transparent	Transparent

1.6 LIQUID-STATE VISCOSITY OF MATRIX MATERIALS

The liquid-state viscosity is another important criterion for matrix material selection since it determines the effectiveness of the mixing process and the resulting distribution of dispersions. Rather than an accurate value in poise (whose determination was too involved), relative data were obtained by measuring the time required for a given amount of liquid to flow through an orifice. All tests were carried out at 82.5 ± 0.5°C, which was considered the minimum mixing temperature in the flight experiment. The results, which represent averages of several experiments, are given in the table below. The relative viscosity is defined as $\frac{\eta_x}{\eta_w} = \frac{d_x t_x}{d_w t_w}$ where x refers to the material and w to water. η is the viscosity and d and t are the density and time of flow respectively.

Accordingly after correcting for density, Cerrobend has 9 times the viscosity of water, while In-Bi is eight times more viscous. Burtonite and paraffin have the same viscosity, somewhat higher than water.

Material	Time (Seconds)	Relative Viscosity
Water	15.48	1.0
Cerrobend	15.265	9.1
In-Bi (66/34)	13.72	7.6
Burtonite 1.5%	19.4	1.3
Burtonite 2%	20.4	1.3
Burtonite 3%	20.7	1.3
Paraffin	19.4	1.3

1.7 SOLID-STATE PROPERTIES AND HANDLING OF BURTONITE AND PARAFFIN.

Paraffin is adequately hard at room temperature. Burtonite is a gel with a consistency that depends upon concentration and temperature. The consistency was determined numerically by measuring the load required to cause penetration of a 0.6-inch diameter cylinder. The load carrying capability in gm/cm^2 at room temperature and 3°C for increasing concentration is given in the following table and is illustrated in Figure 1-4.

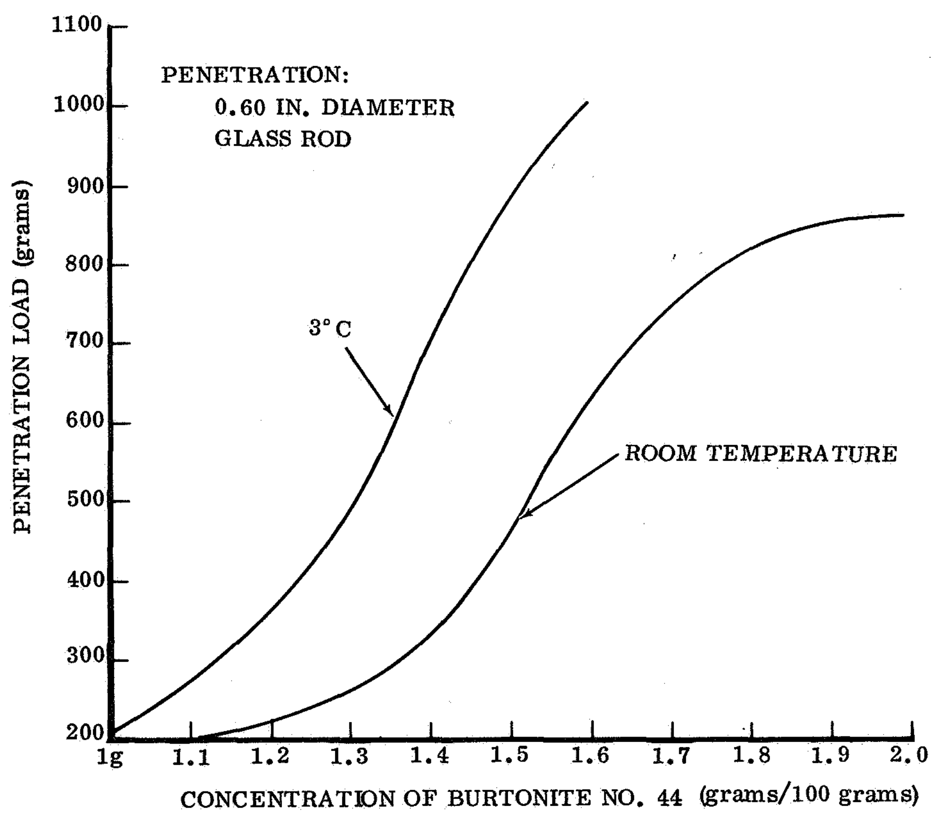

Figure 1-4. Supportive Strength of Burtonite Concentrations at 3°C and Ambient Temperature

Burtonite 44 (% Concentration)	Max Specific Load (gm/cm^2) R.T.	3°C
1	< 78	115
1.1	< 78	101
1.2	115	78*
1.3	140	271
1.4	182	275
1.5	260	495
1.6	355	570
2.0	472	-
3.0	1,050	-

At the previously selected concentration of 1.5%, the load carrying capability of 1/2 lb per cm^2 at R.T. is more than adequate for handling after sample return. However, as a gel it has practically no tensile strength and will have to be transferred from the cartridge into a transparent container. The transfer by flash heating of the open-end cartridge was performed without any difficulty in the laboratory.

The same method of removal from the cartridge may be used for paraffin, as cutting of the cartridge may produce fractures in view of its high solid-state brittleness.

* Discontinuity unexplained; value at 3°C correct.

SECTION 2

EVALUATION OF REINFORCEMENT MATERIALS

2.1 CANDIDATE MATERIALS

For lack of a more descriptive term, the words "reinforcements" and "dispersions" are used alternately for all types of matter to be dispersed in the matrixes. The initial list of candidate materials to be evaluated was:

a. Chopped metal wires

b. Chopped glass filaments

c. Chopped boron filaments

d. Whiskers

e. Metallic microparticles

f. Oxide microparticles

g. Macroparticles

h. Immiscible liquids

i. Gases

The objectives of these materials as dispersions in various composite materials are summarized in Table 2-1.

Evaluations were carried out for materials a through f as they are discussed in Sections 2.3 through 2.8. Macroparticles and immiscible liquids were excluded, since they were evaluated by Cornell and TRW, respectively. The evaluation of gases was confined to dispersion techniques, discussed in Section 4.5.

2.2 EVALUATION PROCEDURES AND CRITERIA

The criteria for fiber reinforcement selection and surface treatment, in the order of the evaluation and elimination procedure, were:

a. Chemical compatibility with the matrix

b. Wetting by the liquid matrix

c. Adherence of the solidified matrix

Table 2-1. Types and Objectives of Candidate Dispersion Materials

No.	Dispersion	Objective	Eval. Sect.
1	Chopped Metal Wires	High-strength composites	2.3
2	Chopped Glass Filaments		2.4
3	Chopped Boron Filaments		2.5
4	Whiskers		2.6
5	Metallic Microparticles	Nucleation and microstructure control	2.7
6	Oxide Microparticles	Dispersion-stabilized metals	2.8
7	Macroparticles	Cemented compacts and simulated nuclear fuel elements	—
8	Immiscible Liquids	Simulation of supersaturated alloys	—
9	Gases	Controlled-density materials	
	(9) + (1) through (4)	Materials with high strength/density ratio	—

d. Bond strength between reinforcement and solidified matrix

e. Reinforcement material strength

For microparticles, chemical compatibility and wetting characteristics were taken into consideration; for metallic particles, the potential effect upon microstructure formation (nucleation); and for oxide particles, their potential effectiveness as stabilizers of the cold-worked matrix.

In the following sections, the evaluation of these criteria and the related experiments are described in detail for each of the dispersion materials identified in Section 2.1 (materials a to f).

2.3 METALLIC REINFORCEMENT MATERIALS

Initially, all investigations and experiments were based on the Cerrobend matrix. Additional experiments were carried out with the In-Bi matrix in the latter part of the evaluation.

2.3.1 CHEMICAL COMPATIBILITY. The chemical compatibility of candidate metals was assessed by judgment. During experimentation, none of the so-selected materials showed any chemical reaction with Cerrobend and In-Bi in the solid and liquid state, with the exception of galvanized wires in which the zinc coating started to dissolve in In-Bi at 280° F.

2.3.2 WETTING AND ADHERENCE. Wetting characteristics were determined by dipping of wires or sheet strips with various surface conditions in the liquid matrix and observation of the behavior of the liquid film after removal. Wettability was expressed in % by judgment (0% = non-wetting, 100% = fully wetting).

Samples that showed adequate wetting characteristics were slowly cooled; after solidification of the matrix film, adherence was tested by scraping with a cutting tool. Adherence was likewise expressed in % (0% = peeling-off, 100% = complete bond with the substrate).

The results of initial wetting and adherence experiments carried out with metal strips are summarized in Table 2-2. Surface treatments were applied to the point where 100% wetting and adherence was obtained. Experiments with various wires and more extensive surface treatment variations are summarized in Table 2-3.

2.3.3 SINGLE FIBER BOND STRENGTH. In ground experiments, the effectiveness of reinforcements in a composite casting cannot be determined since gravity precludes the maintenance of dispersion. However, theoretical predictions can be made on the basis of the shear strength between filaments and the solidified matrix that can be obtained in laboratory tests.

For the single-filament bond test, filaments were cast into the matrix at various depths, using a 0.35-inch-diameter cylindrical mold. Tensile tests were carried out at room temperature and 0°C. The shear strength was determined from the cylindrical contact area of the filament and the maximum load according to:

$$F_S = \frac{L}{\pi d h} \text{ (psi)}$$

where L = maximum load

d = filament diameter

h = depth in matrix

The test apparatus is illustrated in Figure 2-1. The load was applied gradually by dispersing steel shot in the loading bucket and microscopic observations of a filament mark at the casting surface were made. The maximum load was obtained from the weight of the filled bucket at the moment where the first movement of the filament was observed.

Table 2-2. Wetting and Adherence Experiments, Metal Strips

Matrix	Substrate	Substrate Surface Condition	Wetting (%)	Adher. (%)
Cerrobend	Aluminum	Degreased	0	-
		Degreased + SS Flux	0	-
	Tin	Degreased	100	100
	Silver	Degreased	100	100
		Degreased + SS Flux	100	100
	Copper	Degreased	0	0
		Degreased + SS Flux	100	100
	Nickel	Degreased	80	0
		Degreased + SS Flux	100	100
	Gold	Degreased	90	0
		Degreased + SS Flux	100	100
In-Bi	Aluminum	Degreased	0	0
		Degreased + SS Flux	0	0
	Tin	Degreased	100	100
	Silver	Degreased	100	100
	Copper	Degreased	0	0
		Degreased + SS Flux	100	100
	Nickel	Degreased	25	0
		Degreased + SS Flux	100	100
	Gold	Degreased	90	0
		Degreased + SS Flux	100	100

A refined version of the test apparatus, used in the latter part of the experiments, is shown in Figure 2-2. It eliminated clamping pressure at the casting as well as at the wire end (spooled end). Boron filament ends were held in a clamped rubber stopper to preclude fracture.

The test results for steel, copper, Cu-Be and boron filaments with various surface treatments are summarized in Table 2-4. The data represent averages of several tests carried out with each material and surface condition.

Table 2-3. Wetting and Adherence Experiments, Reinforcements and Dispersion Materials

Treatment	Carbon Steel	Music Wire	Galv Steel	Stainless	Cu	BeCu	Glass	B	Al_2O_3 Whisk	Al_2O_3 (Alon)
A. As is	→	→	→	→	→	→	→	→	→	→
B. Degreased	○	●	→	○	→	→	○	●		
C. De-oxidized	○		→	→	●	●				
D. + Fluxed	●	●	○	●	●	●				
E. B + C + D	●	●	●	●	●	●				
F. Coated/Plated	●		→		★			●	●	
G. C + F	●		→		★		○			
Resulting Bond										
Adherence	●	●	●	●	●	●	●	●	●	
Diffusion	●		●	○	●	●		○		

→ No wetting

○ Some wetting

● Wets

★ Additional improvements

High bond strength was obtained with tinned copper (5163 psi) and Cu-Be wire (3390 psi) as well as with boron filaments (3612 psi). An examination of Table 2-4 shows that there appears to be no correlation between contact area (depth) and shear strength; in fact, higher cast-in depths produced generally lower values, while the highest values were invariably obtained with a depth of only 40 to 50 mils. This implies that nothing is gained by high fiber length and that an L/D of approximately 10 is an optimum. Such conclusions are, however, premature and a more extensive experimental evaluation is indicated.

2.3.4 MECHANICAL PROPERTIES OF REINFORCEMENTS. For practical applications, the primary criterion for reinforcement selection is its strength and, to a lesser degree, its elastic properties. Even though only of secondary importance

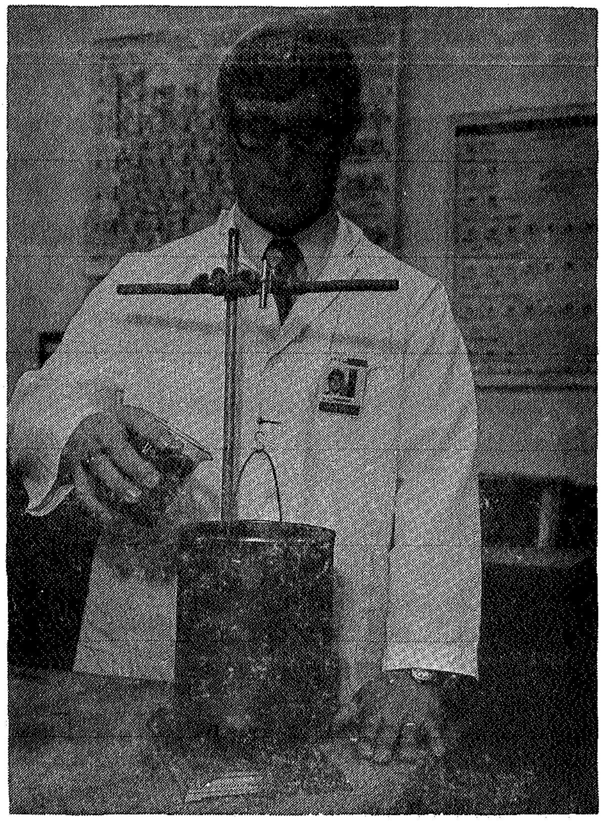

Figure 2-1. Single-Filament Bond Test

for the Apollo 14 experiments, the mechanical properties were also taken into consideration for reinforcement selection. They were obtained by tensile tests (wires) and from the literature. The data are summarized in Table 2-5, which includes, for comparison, the reinforcements discussed in Sections 2.4, 2.5, and 2.6.

2.4 CHOPPED GLASS FILAMENTS

The consideration of glass filaments was prompted by the high strength of thin glass fibers (400,000 to 500,000 psi) and their low cost.

While glass presented no problems as to chemical compatibility, the wetting and bonding characteristics were negative. It was attempted to improve these properties in two ways:

a. Thermal treatment of high-lead glass

b. Metallic coating of conventional E-glass.

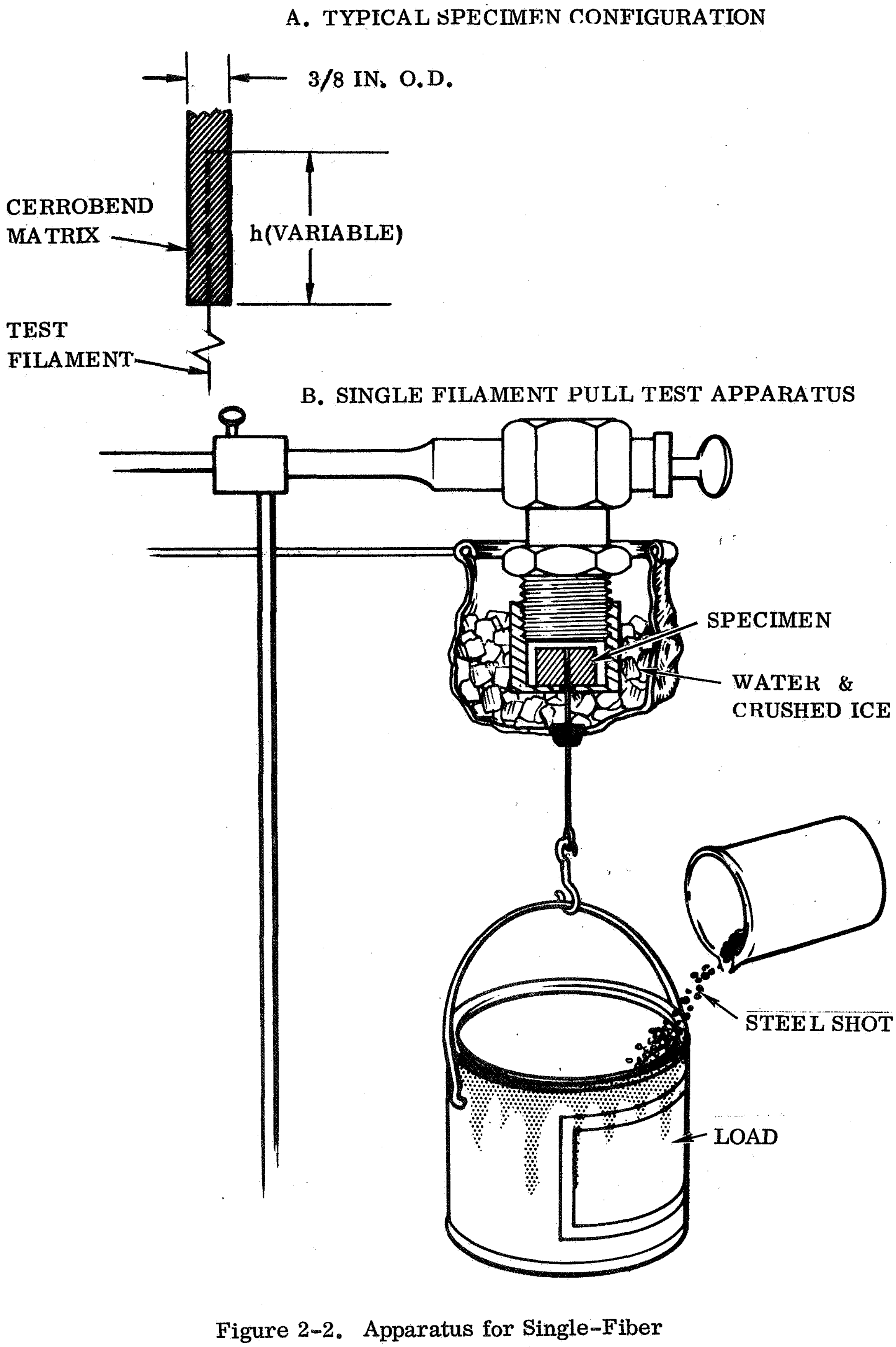

Figure 2-2. Apparatus for Single-Fiber Bond Strength Tests

Table 2-4. Single Filament Bond (Pull) Tests, All-Cerrobend Matrix

Filament Material	Dia (Thick) (mil)	Form	Treatment: Degrease	Deoxidize	Fluxcoat	Coat (Cer)	Cast Depth (mil)	Test Temp. (°C)	Shear Strength (psi)
Stainless Steel	6	RD	x	-	-	-	1000	22	~114
Carbon Steel	3	RD	x	-	-	-	1000	22	~192
Copper	29	RD	x	x	x	x	120	22	1,746
Copper	(25)	FL/TW*	x	x		x	110	22	1,490
Copper	(25)	FL/TW	x	x	x	x	77	22	1,963
Copper	(25)	FL/TW	x	x		x	78	0	2,293
Copper (Tinned)	40	RD	x	x		x	52	0	5,163
BeCu	40	RD	x	x	x	x	80	0	2,500
BeCu	5	RD	x	x	x	x	115	22	1,475
BeCu	5	RD	x	x	x	x	95	22	1,417
BeCu	5	RD	x	x	x	x	40	22	3,390
BeCu	5	RD	x	x	x	x	45	22	1,890
BeCu	5	RD	x	x	x	x	95	22	2,200
Boron	4	RD	x			x	80	22	3,612
Boron	4	RD	x			x	80	22	830

The high-lead glass filaments were prepared by a commercial glass blower. They were heated to various temperatures until the glass turned black, indicating a segregation of the dissolved lead in metallic form. It was assumed that the leaded surface would be more compatible with the matrix metal. However, wetting and bonding characteristics were only slightly improved, while single-fiber strength tests showed no improvement. In addition, the thermal treatment may reduce the strength. The approach was therefore abandoned. It may, however, be reconsidered later as a means of pre-treatment for metal-coating of glass fibers.

*Flat-twisted (round wire rolled and twisted).

Table 2-5. Mechanical Properties of Reinforcements

Reinforcement Material (all wires cold drawn)	Tensile Strength (10^3 psi)	Elastic Modulus (10^6 psi)
Stainless Steel Wire (6 mil)	313	28
Music Wire (3 mil)	377	29
Copper Wire (10 mil)	50	17
Cu-Be Wire (5 mil)	153*	19
Nickel (Spring Wire)	130	30
Nickel Alloys (Max.)	200	32
Glass Filaments (0.5 mil)	450	10
Boron Filaments (4 mil)	400	60
Graphite Filaments	500	100
Sapphire Whiskers	500-3,500	60-150
SiC Whiskers	2,000-6,000	80-150
BeO Whiskers	1,800	50

* 3/4-hard Cu-Be wire as used in flight experiments.
Max. full-hard strength = 190,000 psi.

For the generation of a metallic interface, coating experiments were carried out with silver and copper since both materials provide good wetting and bonding characteristics. Initial experiments were performed on glass slides, followed by filaments of 0.080 and 0.005-inch diameter. Coatings with both materials were achieved by chemical deposition methods. However, plain silver did not adhere. With copper, varying results were obtained; in some cases excellent bonding to the glass was obtained, while other experiments under the same conditions produced inadequate adherence. An effective bond between the coated glass and the matrix metal was obtained only when the coating was fully de-oxidized. Single-filament tensile tests were inconclusive as all broke prematurely at the contact point with the casting surface; time limitations did not permit refinement of the testing technique.

Best results in coating adherence and single-fiber tensile tests were obtained with a freshly drawn filament, prepared by Narmco Division of Whittaker Corp., which was coiled on a large-diameter drum. Whether this result was due to glass composition, cleanliness, or freedom from cracks was not determined. It indicates, however, that by proper preparation, glass may be an effective reinforcement. It was concluded that:

a. The adherence of the coating depends on the cleanliness of the glass filament, including the freedom from adhering gases.

b. For an effective bond between the fiber and the matrix metal, the coating has to be "bare"; i.e., free of oxides. (A stainless steel flux is a good de-oxidizer and sealer.)

c. The strengthening effectiveness in a composite is highly dependent upon the mechanical surface condition of the glass filament; i.e., the freedom from cracks. (Most commercial fibers have a network of surface cracks.)

In view of the difficulties and the indicated need for more extensive R&D, glass filaments were eliminated from the Apollo 14 experiments.

2.5 BORON FILAMENTS

Chemical compatibility appeared to present no problems, even though dissolution of boron filaments was observed in parallel experiments at MSFC. Wetting proved to be negative and could not be improved by chemical surface treatments. This indicated the necessity of coating. Copper and silver coatings were applied successfully by chemical deposition, as well as silver coating by means of sputtering. Figure 2-3 shows a silver-coated boron filament (100X). All coatings showed good adherence. However, as with the silver and copper coated glass filaments, good wetting and bonding characteristics with the metal matrix were obtained only after a de-oxidation treatment of the coating.

Single filament tests were performed only with degreased, uncoated boron filaments, which produced a high shear strength of 3312 psi. Whether this high strength is due to surface-energy bonding or a mechanical interlocking effect of the irregular surface configuration of the filament providing high shear resistance, or due to a combination of both is unresolved.

Chopped boron filaments are judged very promising. However, experiments were discontinued to avoid duplication of the work in progress at the time at MSFC.

2.6 WHISKERS

Initially, three types of whiskers were considered for the flight experiments:

a. Al_2O_3-α (sapphire) whiskers

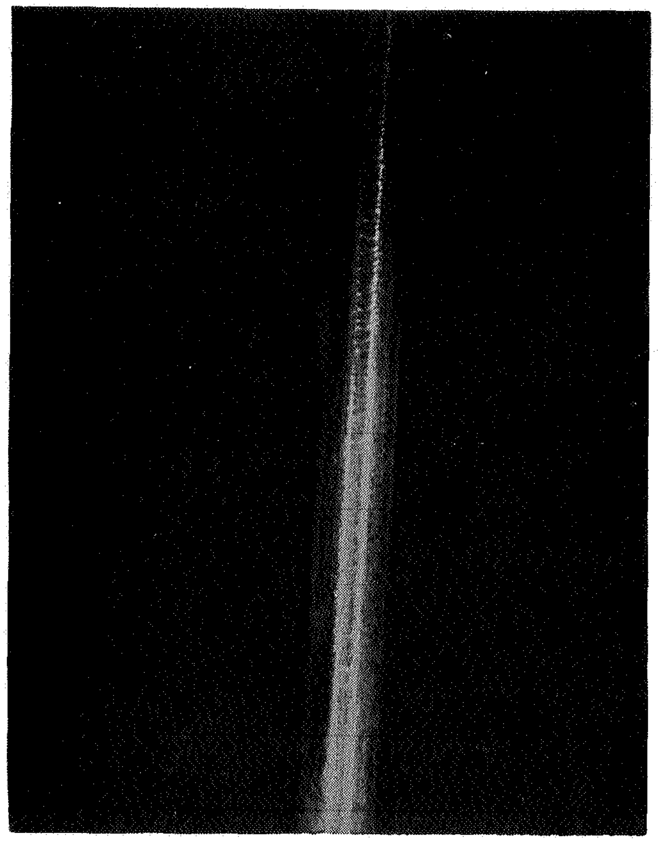

Figure 2-3. Silver-Coated Boron Filament (100×)

b. Mixed sapphire and AlN whiskers

c. SiC whiskers

The investigation of silicon carbide whiskers was carried out by MSFC. The mixed whiskers were eliminated after microscopic examination, since they proved to contain an excessive amount of very short, powderlike whiskers, ineffective as reinforcements (average length less than 50 microns). The evaluation was, therefore, confined to pure sapphire whiskers.

The sapphire whiskers, on hand from previous contract work, proved to be very clean and of appreciable length, varying from approximately 10 to 120 mils, with some as long as 200 mils. Assuming an average diameter of 8 microns (approximately

0.3 mil) the average L/D was in the order of 200. Their physical properties, according to the manufacturer's specification were:

Density	3.97 gm/cm^3
Diameter	1 to 30 microns
Length	180 to 2500 microns
Strength	0.5 to 3.5 x 10^6 psi
Elastic Modulus	60 to 150 x 10^6 psi

Chemical compatibility, wetting, and coating experiments were carried out with a flat sapphire disk and with whiskers. Chemically, sapphire is fully compatible with the metal matrix. Wetting characteristics were negative and called for surface treatment.

Chemical surface cleaning did not improve the wetting characteristics. Coatings on untreated whiskers proved unsatisfactory. After chemical cleaning, small samples of whiskers were successfully coated with silver by sputtering. For the quantities required, special devices required for whisker agitation during sputtering could not be built within the time limitations. Therefore, several chemical deposition processes were evaluated. Successful coating with copper by electroless plating was achieved with the following process:

a. Clean

Solution: 96% H_2SO_4
4% HNO_3

Boil in solution for 5 minutes

Purpose: to remove organic matter left on whiskers from classification process.

b. Rinse in distilled water and decant until litmus test shows no acid (at least 3 times).

c. Activate

Solution: 25% activator 9070*($SnCl_2$ + $PdCl_2$)
20% HCl
55% distilled water

Immerse, agitate for 8 minutes at room temperature.

* MacDermid, Inc., Waterbury, Connecticut

d. Rinse in distilled water.

e. Accelerate

Solution: 10% solution 9071*

90% distilled water

Immerse and agitate for 2 minutes at room temperature.

f. Rinse in distilled water

g. Coating

Solution: 10% solution 22A†

10% solution 22B†

80% distilled water

h. Rinse in distilled water.

i. Rinse in alcohol.

j. Store in alcohol.

Even though never tried, it appears advisable to store the whiskers in alcohol to the time of use, and to remove the alcohol shortly before composite preparation by decanting and drying.

Under the microscope, small samples of whiskers coated by the described process showed 100% coating with a shiny surface (Figure 2-4). Consequently, it was decided to process the entire supply of sapphire whiskers, an amount barely enough for the flight samples. To assure a thorough cleaning, the batch was boiled in the cleaning solution for several hours; for unexplained reasons, the whiskers decomposed completely during this treatment into small particles. Replacement sapphire whiskers were not readily available, and the preparation of new whiskers was precluded by time limitations. The use of sapphire whiskers had to be abandoned and SiC-whiskers prepared at MSFC were substituted.

2.7 METALLIC MICROPARTICLES

One of the potential applications of the zero-g mixture stability is the dispersion of metallic microparticles in alloys to act as nuclei for the formation of fine-grain cast microstructures. From the start this concept was not very promising for the flyback experiments in view of the eutectic composition of the candidate base alloys. Nevertheless, some laboratory experiments were carried out. At the suggestion of

* MacDermid, Inc., Waterbury, Connecticut
† W. R Hatch & Co., Azusa, California

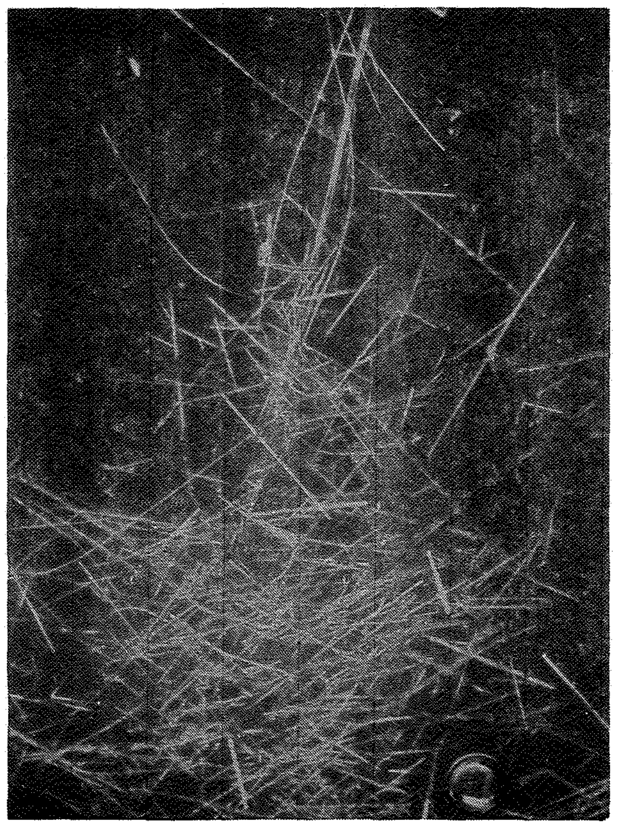

A. UNCOATED

B. SILVER-COATED

Figure 2-4. Sapphire Whiskers

Dr. Tiller, pure copper particles of approximately 10 microns size were used because copper appeared to be an effective activator for the candidate alloys. The de-oxidized particles were mixed with the liquid matrix and the mixture cast on a glass plate. Since the gravity of copper is somewhat higher than both Cerrobend and In-Bi, the particles settled at the metal-glass interface, which was evaluated for microstructural effects after solidification. Even at slow cooling rates, no effect was observed and the concept was deleted from the list of candidate flight experiments.

2.8 OXIDE MICROPARTICLES

Tests were made to evaluate Alon powder as a matrix reinforcement for Cerrobend. Alon is a fine light powder of Al_2O_3 (particle size approximately 0.1 micron). It was thought that the Cerrobend matrix properties could be enhanced by dispersing fine particles in it to improve creep resistance and to control grain growth, size, and structure.

Attempts to disperse the powder into the metal matrix were unsuccessful. No interaction occurred even when the system was heated and stirred vigorously. The tests were conducted under vacuum also in attempts to remove and/or avoid interference by gases absorbed on the large surface area of the particles. Vacuum was applied and the Alon-Cerrobend system was simultaneously heated with active shaking. The Alon remained as a separate phase above the Cerrobend. No change in the Cerrobend properties was evident. It was concluded that particles with improved wettability, which would disperse at zero-g, might still be useful and the commercially available material could have application for dispersion-stabilized alloys, but no further experiments related to Apollo 14 could be performed because of time limitations.

SECTION 3

COMPOSITE EXPERIMENTS

It should be emphasized that all test data of composites prepared under gravity conditions can only indicate trends due to the necessarily imperfect mixing. Strength data expected under zero-g and perfect dispersion have been calculated in Table 3-1 for Cerrobend-base composite castings with various reinforcement strength and content levels. To account for the effect of the random fiber orientation upon unidirectional strength, a "composite factor" has been introduced, tentatively placed between 0.25 and 0.5. Accurate data for this factor can only be obtained in zero-g experiments.

3.1 COMPOSITE CASTING TECHNIQUES UNDER GRAVITY CONDITIONS

An aluminum split mold was machined for the preparation of standard "dog bone" tensile specimens with a gauge diameter of 0.505 inch (Figure 3-1). Cerrobend and In-Bi alloy specimens (Tests 1 and 3 to 7 in Table 3-2) were cast in the mold, which was provided with additional external risers to ensure void-free castings. The mold was pre-heated to a temperature slightly above the melting point of the alloy being cast, and the molten metal was poured into the riser openings in the mold while it was in a horizontal position. The hot mold was then rapidly cooled by submerging it in ice water to a level just below the external risers. X-rays were made of the cast specimens to verify that no serious porosity existed that could possibly affect test results.

One composite casting specimen was made with the mold in a vertical position. This specimen was a stainless steel wire (313 ksi) fiber-reinforced Cerrobend matrix casting with a fiber content of 27% by volume (see Table 3-2, Test 2). The casting was made in a vertical position so that the fiber and matrix materials could be alternately added a little at a time to reduce possible porosity. The relatively high fiber content (27%) prevented free movement of the fibers due to packing; therefore, the materials could not be mixed by stirring. The fractured tensile specimen is shown in Figure 3-2.

Due to the quantities of matrix and reinforcement fibers required to prepare specimens in the dog bone mold, subsequent composite casting specimens were prepared in 0.375-inch I.D. glass tubes. The glass tube molds required less materials for specimen preparation; they also made possible the preparation of vacuum castings. Another feature of the glass mold method was that the specimens could be solidified more rapidly resulting in less grain growth. Two composite vacuum castings were prepared with "pretinned" fibers in glass tubes as described above and they were tensile tested with grip-type jaws (see Tests 8 and 9 in Table 3-2). However, both of these specimens broke at the jaws. Consequently, a technique was developed to cast

Table 3-1. Calculated Composite Strength and Strength Gain

MATRIX: CERRO ALLOY
F_{TU} = 6000 PSI

REINFORCEMENT: RANDOM CHOPPED WIRES
F_{TU} = 100,000 to 400,000 PSI

Wire F_{TU} (psi)	Wire Content (Vol. %)	Composite Factor 0.5		Composite Factor 0.25	
		Strength (psi)	Gain (%)	Strength (psi)	Gain (%)
100,000	2	6,900	15	6,400	7
	5	8,200	36	6,950	16
	10	10,400	73	7,900	32
	20	14,800	147○	9,800	62
200,000	2	7,900	31	6,900	15
	5	10,700	78	8,200	36
	10	15,400	156●	10,400	73
	20	24,800	313	14,800	147○
300,000	2	8,900	48	7,400	23
	5	13,200	117●	9,400	56
	10●	20,400	238●	12,900	114★
	20	34,800	477	19,800	229
400,000	2	9,900	65	7,900	31
	5	15,700	162●	10,700	78
	10●	25,400	323●	15,400	156★
	20	44,800	645	24,800	313

○ Over double strength

● Feasible experiment regimes

★ Highest assurance of success

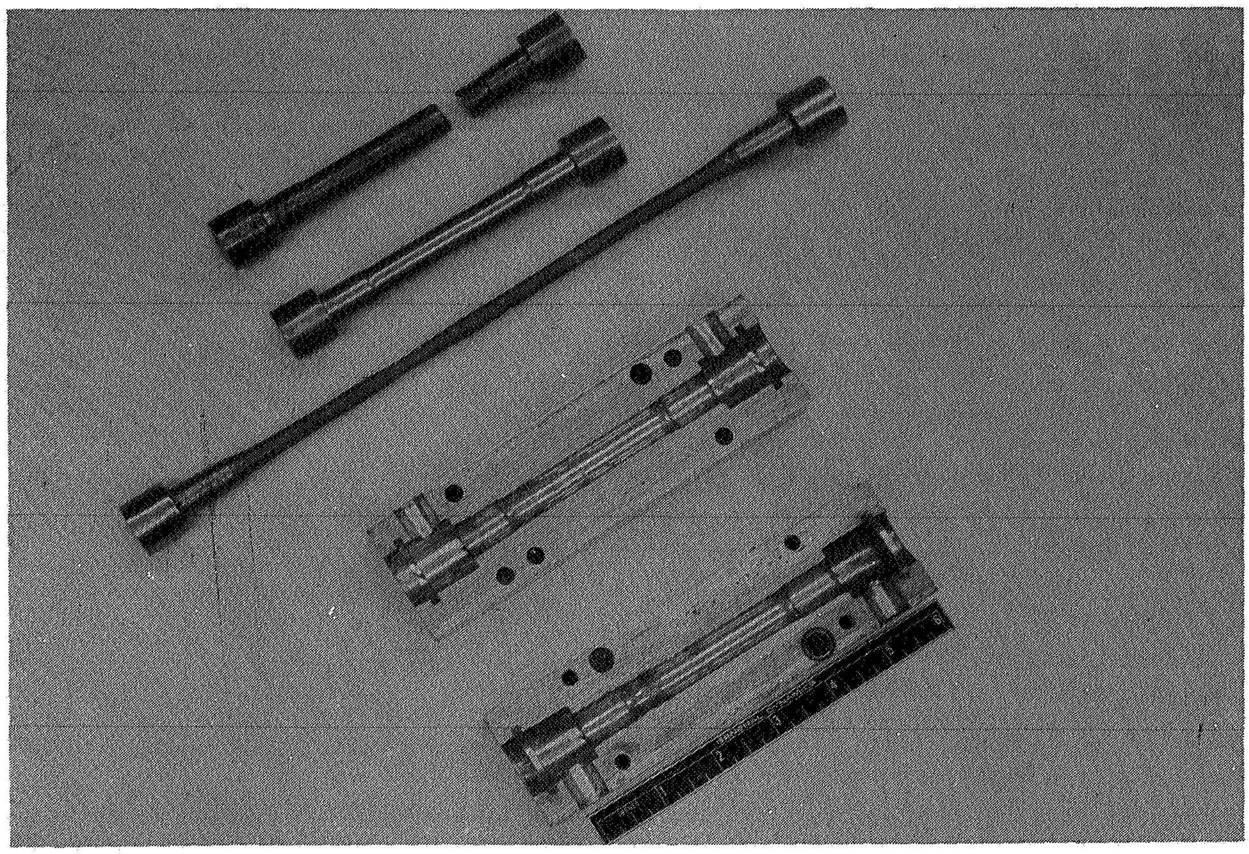

Figure 3-1. Tensile Specimen and Casting Mold

Table 3-2. Tensile Test Results of Cast Matrix and Composite Specimens

Test No.	Matrix Material	Reinforcement Material	Specimen Type	Casting Type	Test Temp (°C)	Ultimate Tensile Strength (ksi)
1	Cerrobend	None	1/2 in. dia. "dog bone"	Air	25	3.134
2	Cerrobend	Steel wire; 27% 6 mil dia. × 190 mil long	1/2 in. dia. "dog bone"	Air	25	2.077
3	Cerrobend	None	1/2 in. dia. "dog bone"	Air	25	2.407
4	Cerrobend	None	1/2 in. dia. "dog bone"	Air	0	6.012
5	Cerrobend	None	1/2 in. dia. "dog bone"	Air	-78	7.509
6	In-Bi	None	1/2 in. dia. "dog bone"	Air	25	1.261
7	In-Bi	None	1/2 in. dia. "dog bone"	Air	0	2.293
8	Cerrobend	Be-Cu wire; 12% 5 mil dia. × 100 mil long	3/8 in. dia. × 6 in. long rod	Vacuum	25	4.135
9	Cerrobend	Cu wire; 12% 5 mil dia. × 125 mil long	3/8 in. dia. × 6 in. long rod	Vacuum	25	6.674

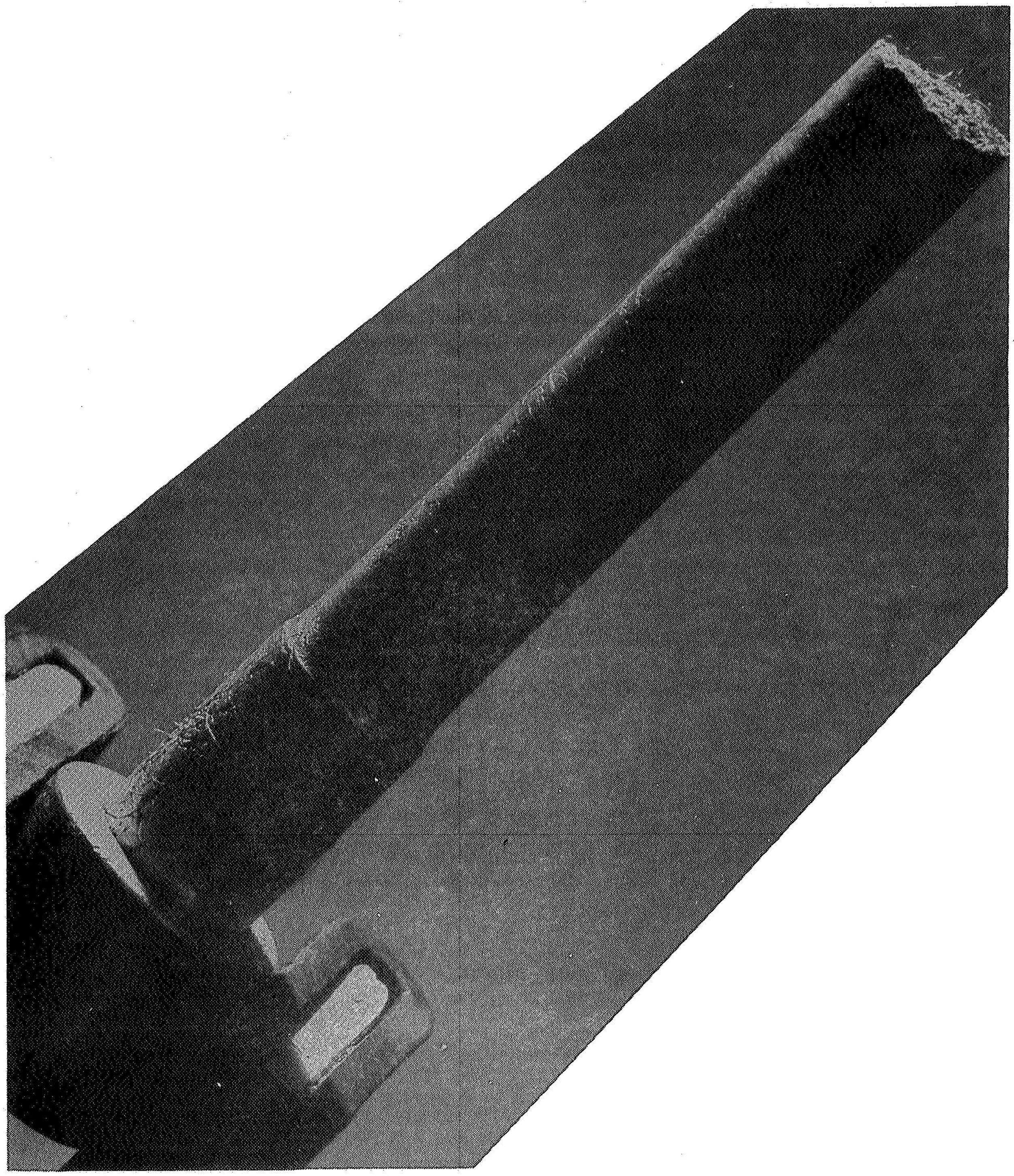

Figure 3-2. Steel Wire-reinforced Cerrobend Tensile Specimen

larger diameter ends on a 0.375-inch-diameter rod-type specimen to simulate a "dog bone" type specimen so that the standard tensile testing jaws could be utilized to prevent stress concentrations in the gripping area. The larger diameter ends were prepared on the specimens by placing each end separately in a cup-type mold and casting additional matrix metal around it. The end was then post-heated enough to just weld the joint together without melting the exposed area of the original composite specimen above the new end. Due to time limitations, tensile specimen preparation was discontinued, so the above technique was not proven out in actual tensile tests.

3.2 TENSILE TESTS

Plans were to conduct a sufficient number of tensile tests on both specimens consisting of cast parent matrix materials and composite castings with various reinforcement fibers to establish valid data for strength evaluations. However, due to time limitations, only a limited number of tensile tests was carried out with composites prepared under gravity conditions. Therefore, the results presented in Table 3-2 are inconclusive. It can be seen, however, that the fiber/matrix bond strength is significant as expected. For example, reinforcement of Cerrobend with Cu-Be and plain Cu fibers, which both exhibit high bond strength (see Table 2-4), doubled the strength at 25° C, as evidenced by comparison of Tests 1, 8, and 9 in Table 3-2. By the same token, the relatively low strength value of Test 2 correlates well with the poor bond strength of steel reinforcements.

3.3 REINFORCEMENT CONFIGURATION AND OPTIMUM COMPOSITE CONTENT

The enhancement of the properties of a material by fibers depends, among other parameters, upon the amount of fibers added and the ratio of their length to diameter (L/D). Very short fibers of low L/D behave like particles. These can be loaded to 50 to 70% of the total volume with retention of the fluid properties of the system. Very long fibers of high L/D either line up in the short capsules used or they entangle themselves so that no dispersion occurs.

Between these extremes, at an optimum loading percent and an optimum L/D ratio, the system retains the properties of the matrix yet is greatly strengthened by the presence of fibers.

Preliminary experiments were performed to evaluate the range of loading and fiber configuration leading to the optimum system. The criteria for percent loading were qualitative for these preliminary experiments and depended on ease of dispersal, lack of matting, and uniformity of distribution. The results showed that about 8 to 12% loading would appear optimum.

More definitive experiments were performed for the optimum L/D ratio. The results represent screening experiments, however, and exhibit trends that may be expected and approaches to a more comprehensive investigation.

Table 3-3 shows the results of mixing polysaccharide solution with various configurations of fibers at constant fiber weight corresponding to about 12% loading by volume. After dispersing the fibers uniformly by shaking the standard prepared gel, it was allowed to set and the settling effect was noted by measuring the height occupied by the fibers in the gel.

Table 3-3. Distribution of Nylon Fiber Configuration in Burtonite No. 44

Size of Filaments (in.)	Total Height (in.) Fibers + Burtonite	Fiber Height (in.)
1/8 x 0.01	3.8	2.25
1/8 x 0.026	3.8	1.60
3/8 x 0.026	3.8	2.30
1/8 x 0.0055	3.8	3.5
1/8 x 0.026	3.8	1.55
1/4 x 0.026	3.75	1.70
3/8 x 0.026	3.8	2.00
1/2 x 0.026	3.8	2.80
3/4 x 0.026	3.8	3.25

The data are plotted in Figure 3-3 The final volume occupied by the fibers is plotted against their diameter at a constant length of 0.125 inch (curve a) and against their length at a constant diameter of 0.026 inch (curve b). The curves show that, as the fibers get longer at constant diameter, they are more extensively distributed through the matrix. Also seen is that for a constant length the distribution decreases with diameter. A crossover point occurs at which the distribution is optimum for a fiber which in this case would be 0.375 inch long and about 0.015 inch in diameter, or L/D = 25.

The nature of the material, the wetting properties, and the nature of the system greatly affect the results because of matting and gas entrainment. These factors were not evaluated in this study.

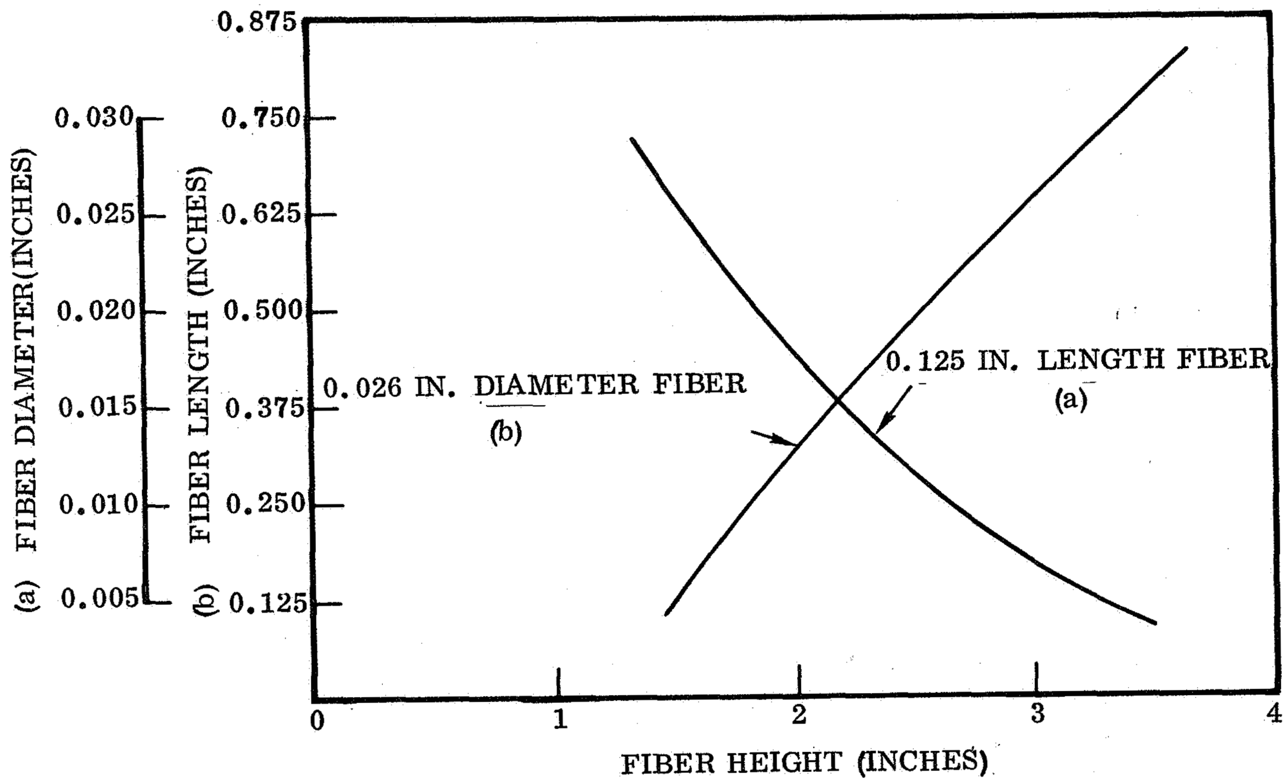

Figure 3-3. Effect of Fiber L/D on Dispersion in Gel Matrix

SECTION 4

SELECTION OF EXPERIMENT MATERIALS

The final decision as to flight experiment materials rested with MSFC; the role of Convair Aerospace consisted of recommendations based on the evaluations and laboratory experiments described in the preceding sections. Documentations were made by way of telephone discussions, teletypes, and conferences at MSFC. They were primarily directed at fiber-reinforced composites and the related component materials.

4.1 METALLIC MATRIX

As outlined in Section 2.1, the eutectic 66% In - 34% Bi alloy with a melting temperature of 73°C was recommended as metallic base material. The initially selected Cerrobend alloy with a melting temperature of 70°C was considered somewhat superior for the following reasons:

a. Higher absolute strength.

b. Higher transition temperature from the plastic to the elastic regime; it exhibits full strength at 3°C, while at this temperature the In-Bi is still in the state of transition.

c. Higher density difference with regard to the selected Cu-Be fibers and, consequently, more pronounced segregation in the ground-processed composites.

The sole reason for the elimination of Cerrobend in favor of In-Bi was the presence of Cd, which was not acceptable according to the command module materials specification. In the opinion of Convair Aerospace, this concern was unwarranted since the toxicity of the small Cd content of Cerrobend (10%) is under the most adverse conditions (overheating and rupture of capsule) at least four orders of magnitude below the toxicity threshold limit value, as outlined in Section 1.4.

4.2 TRANSPARENT MATRIX

On the basis of the evaluations of transparent materials (1.5 to 1.7), Convair Aerospace recommended the use of Burtonite 44 for the following reasons:

a. In contrast to gelatines, which melt between 30 and 32°C, Burtonite remains solid to at least 46°C, compatible with the highest possible temperature in the command module during reentry.

b. Although paraffin has a higher melting point (56°C), it becomes translucent in the solid state, while Burtonite remains perfectly transparent.

On the negative side, Burtonite is a water-base solution which will start to boil if the capsule temperature exceeds 100°C. For this reason, MSFC decided to discard Burtonite in favor of paraffin, with a boiling temperature of 305°C, in spite of its inferior transparency. (Paraffin has been suggested by Convair Aerospace in the past for free-fall experiments.)

4.3 METALLIC REINFORCEMENTS

As outlined in Section 2.3, copper and copper alloys exhibited the most favorable properties for the use as reinforcement materials for both Cerrobend and In-Bi matrixes. Chopped and properly-treated Cu-Be wire was recommended for the following reasons:

a. Excellent wetting characteristics

b. High single-fiber bond strength

c. High wire strength (> 150 ksi)

d. Significant density difference with regard to Cerrobend matrix

e. Immediate availability in various wire diameters

The density difference with regard to In-Bi was less favorable; however, tests showed that even with the small density difference of only 0.1 gm/cm^3 a pronounced segregation is obtained under gravity. In addition, the small density difference was considered advantageous with regard to mixing characteristics under zero-g.

The finally recommended and selected Cu-Be was supplied to MSFC in the form of fibers with 5 mil diameter and 100 mil length, properly cleaned, treated, and coated. Further details are reported in Section 5.

4.4 WHISKERS

Two types of whiskers were recommended:

a. First choice: sapphire (Al_2O_3-α) whiskers

b. Second choice: SiC whiskers

Both types had to be coated with copper for wettability. Sapphire whiskers were considered superior for the following reasons:

a. High L/D (Length up to 200 mils)

b. Surface smoothness

c. Superior adaptability to copper coating.

However, the only available supply of sapphire whiskers, barely sufficient for experiment sample preparation, was lost due to a mishap during surface treatment. Therefore, MSFC had to resort to the use of SiC whiskers, available in ample quantities. For future experiments, it is recommended to return to sapphire whiskers, which may have to be procured from Britain since the U.S. supply of high-grade sapphire whiskers is exhausted and new production is not planned at this time.

4.5 GASES

Several experiments were planned to produce metallic foam and fiber-reinforced metallic foam, representing the addition of gas to the matrix metal or metal-fiber composite. Such experiments appeared promising, particularly for fiber-reinforced metal foam, as it has been demonstrated that the gas bubbles are trapped in the fiber network enhancing stable dispersion, as illustrated in Figure 4-1 (laboratory experiments under g condition).

Argon gas was recommended and selected for the experiments because an inert gas precludes oxide formation in the metallic matrix. (Laboratory investigations carried out after Apollo 14 experiments showed that a small addition of oxygen to the inert gas is desirable, as it stabilizes the bubble walls (interfaces) and reduces coalescence between bubbles).

Figure 4-1. Gas Bubbles Trapped in Fiber Network

SECTION 5

PREPARATION OF FLIGHT SAMPLE MATERIALS

5.1 MATERIALS

The matrix material used for the flight samples consisted of an eutectic 66% In — 34% Bi alloy melting at 72° C, purchased from Indium Corporation of America. This alloy was an alternate choice over Cerrobend alloy, which earlier had aroused concern over a possible toxicity problem because of its cadmium content.

The reinforcement material for the matrix was composed of 0.005-inch-diameter Berylco 25 wire QQ-C-530 cond. 3/4 hard from E. Jordan Brookes Company, Los Angeles, California. This is an alloy of copper strengthened with about 2% beryllium. This wire was chosen for its tensile strength, which was 153,000 psi in the 3/4 hard condition.

5.2 TREATMENT AND COATING

The matrix material, In-Bi alloy, was used in the condition as received by simply melting the necessary quantity into an appropriate container.

The Cu alloy normally has a coating of cadmium which is required by the wire drawing process. The as-received Cd-coated wire is not wet by either Cerrobend or In-Bi so the coating must be removed. Furthermore, bare copper quickly forms on its surface an oxide layer which forms a barrier to wetting by the matrix material. To be used successfully as a reinforcement material, therefore, it was necessary to remove the Cd coating from the wire and replace it with a wettable surface, which in this case was the matrix material itself. This was done in a continuous process as shown in the photograph, Figure 5-1, and sketched in Figure 5-2.

The wire is received on the spool (A) which is placed above the U-tube (B). The wire is led off this spool into a bath of 10% nitric acid in the U-tube. The nitric acid dissolves the cadmium from the wire, which is drawn through the solution at a rate sufficient to ensure complete removal of the cadmium.

The wet wire continues its course into another U-tube (C) in which it is fluxed and coated with alloy. The flux that was found best for preparing the surface for rapid, complete, and certain wetting was Lloyd's Stainless Steel Soldering Flux, Johnson Manufacturing Company, Mt. Vernon, Iowa. This liquid flux layer floats on the surface of the In-Bi alloy, which is kept in the molten state by surrounding the U-tube with a hot water bath. The cleaned and fluxed wire thus enters the molten In-Bi alloy

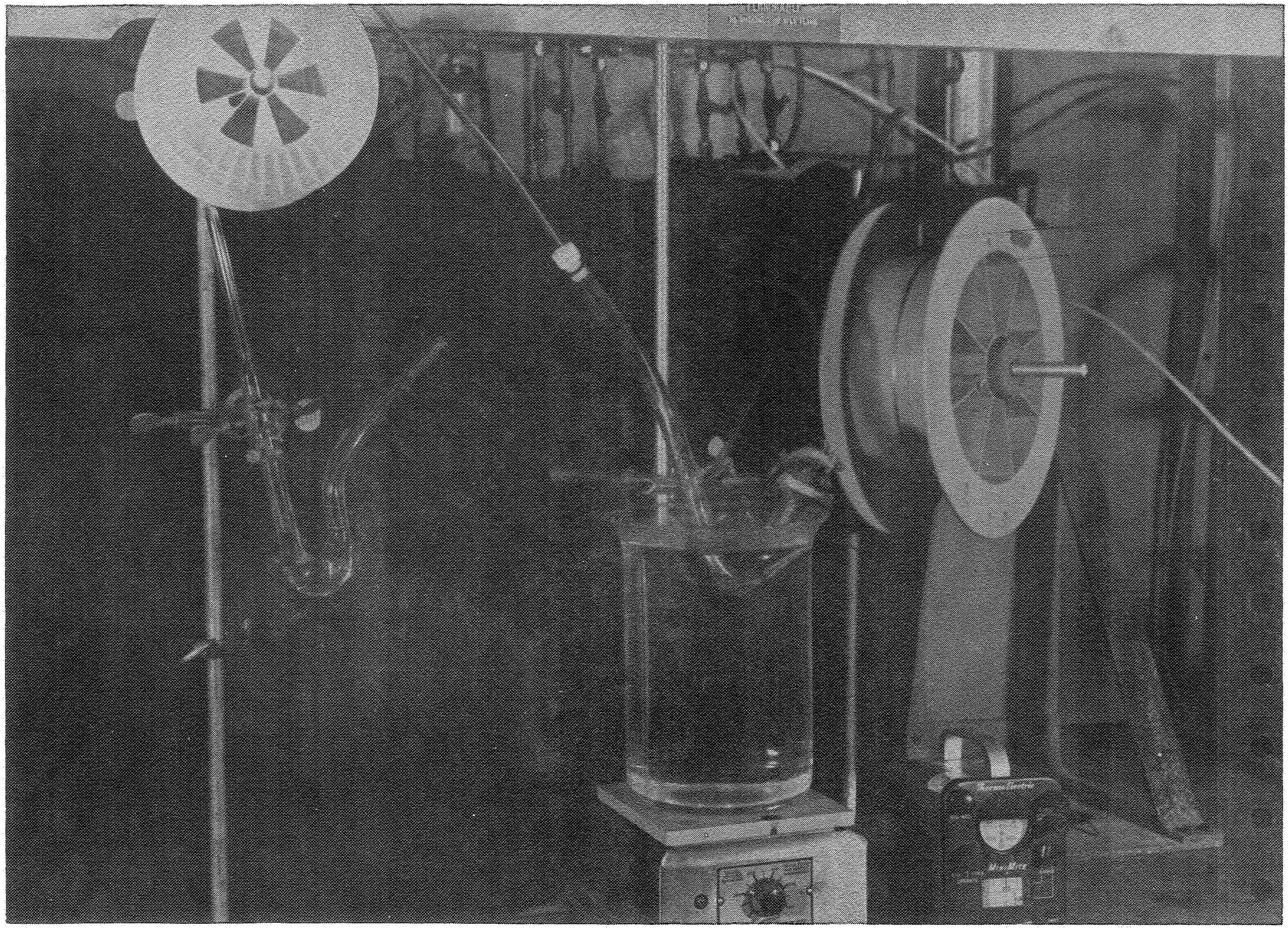

Figure 5-1. Apparatus for Continuous Cleaning and Coating of Wire

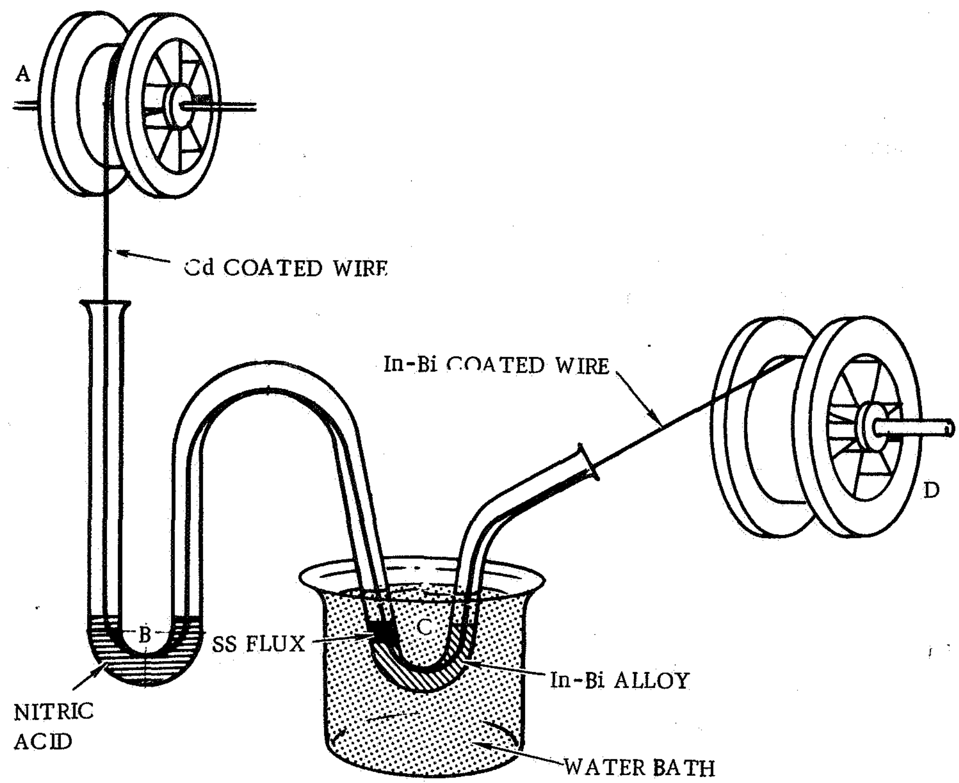

Figure 5-2. Sketch of Test Apparatus

before any exposure to the atmosphere so that the alloy wets it completely. The wire coated with fused alloy leaves the bath and is cooled in the atmosphere to provide an In-Bi alloy-coated wire which is collected on a receiving spool (D).

The rate of cleaning, fluxing and wetting is controlled by the rate of solution of the Cd coating. This rate in turn is regulated by the concentration and depth of acid in U-tube B and amounts to 2 to 4 inches per second.

5.3 CUTTING THE FIBERS

The desired length of the reinforcement fibers was 0.1 inch. Because an automatic machine was not available to prepare the large number of short fibers, the cutting was accomplished with a sheet metal shear and wire strands as follows.

The wire was wound over aluminum foil on a flexible cardboard frame, as illustrated in Figure 5-3. When the desired number of turns (100-200) was wound onto the card, adhesive tape was placed at the edges to keep the strands in place. The wires were then enclosed in the excess foil, the foil rubbed tightly over the wires and the flexible cardboard frame removed to form flat packages about 1.5 inches wide and 10 inches long. The foil served to hold the wires in place during cutting and to assure uniform fiber length. The fiber length was controlled with a stop installed at the shear. After

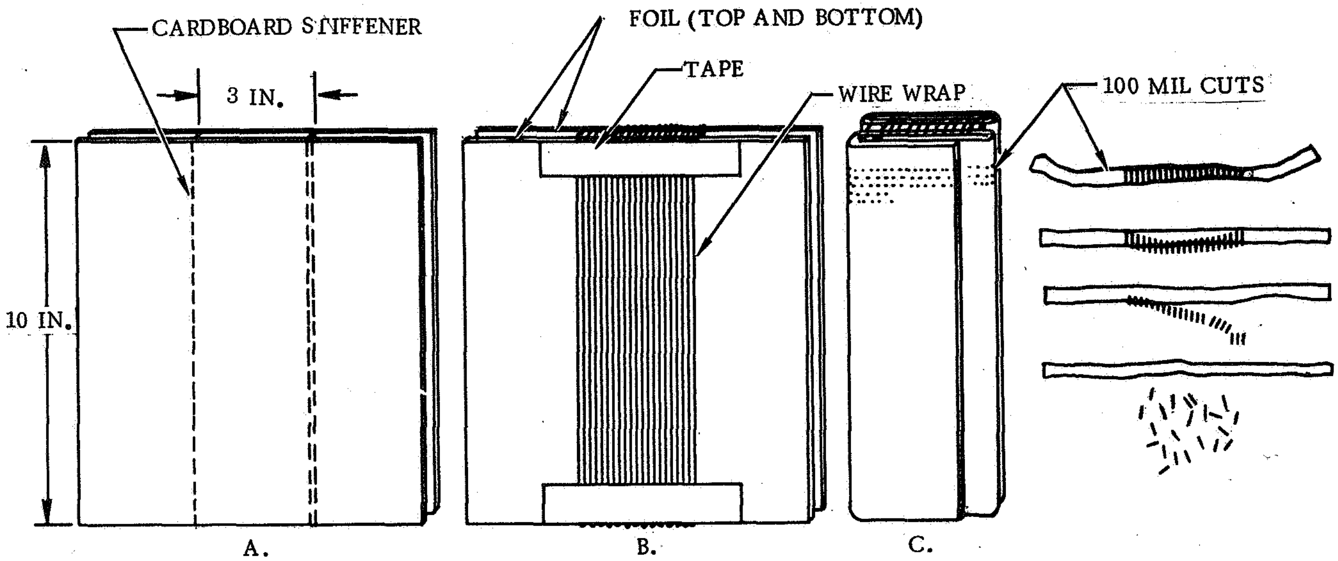

Figure 5-3. Method of Cutting Fibers

cutting, the fibers separate easily from the aluminum foil. With this method, the desired fiber length of 100 mils was maintained within 10%.

One gram of 100-mil Cu-Be fibers contained approximately 3500 individual fibers; consequently, the seven grams used in sample 5 represented approximately 25,000 fibers.

5.4 SAWING THE FIBERS

Another method used to obtain the 0.1-inch fiber consisted of threading the wire strands cut from the cardboard through shrink tubing and cutting to size on a diamond saw. However, the shrink tubing contaminated the fibers. The product was also contaminated with In-Bi and Cu-Be dust. The method as performed was slow, but by using an air blast and automation the most accurately dimensioned fibers could be produced.

5.5 DISPOSITION OF MATERIAL

The In-Bi alloy and the chopped fibers coated with the alloy were sent to MSFC, which provided the facilities for preparing the samples and for loading and encapsulating the materials for the ground and flight experiments.

SECTION 6

INVESTIGATION OF MIXING TECHNIQUES

Experiments were conducted to investigate and develop methods of mixing solid and fluid materials in zero gravity. Three motion pictures were produced in the course of this investigation. The first served as a basic tool and also to document the results. The second, which utilized the results of this first study and other considerations, was filmed to delineate the methods to be used and the expected effects of material mixing for the midcourse (flyback) experiments in space manufacturing.

Both of these motion pictures employ the equal density simulation of the orbital null-gravity condition. Models of the actual experiment capsule (or at least its internal configuration) were fabricated of transparent plastic and filled with mixtures of solid particles and controlled density liquid in which the solids neither sank nor floated. The contents of the capsules were observed by motion picture cameras operating at different speeds up to 400 frames per second in order to slow down the movement of the materials so that the patterns could be optically assimilated. This assimilation kept pace with the experimentation. That was achieved by immediate (10 minutes) development and projection of the motion pictures. The camera for most of the investigation was mounted on the capsule (or vice versa) and moved with it, thus revealing the true flow patterns relative to the capsule. The experiments immediately demonstrated that rotational oscillation about an axis not parallel to the cylindrical capsule axis could create vigorous agitation of the contents. The internal flow patterns were most clearly demonstrated with only a few particles present, but were effective with particle or simulated reinforcement fractions up to and above that recommended for the flight experiments. The results, documented in the first movie, led to definite recommendations on "How to Shake a Capsule," documented in the second movie.

Briefly, it was recommended that the capsule be oscillated about an axis perpendicular to its centerline, through the largest angle and at the highest frequency available, these having been selected to avoid general rotation of the mix about the capsule axis and to maximize the general turbulence. It was also recommended that the oscillations be gradually slowed in order to damp out the more violent eddies and thus avoid centrifugal separation of the different density materials in the actual capsule. Further recommendations of this second motion picture, such as bumping the ends of the capsule in order to break up clumps of reinforcement material, were derived from sources other than the equal density liquid mixing tests.

The third motion picture was a documentary summary of zero-gravity mixing and liquid behavior as it pertains to space manufacturing. Specifically, it shows pictures to support a description of:

a. How water squeezed out of a sponge or a ball released from the hand falls in normal gravity but not when in orbit.

b. A summary of the astronaut's capsule handling procedure.

c. The behavior of reinforcement materials in orbital versus gravitational conditions.

d. How liquid foams form and gravity tends to destroy them.

e. Some possibilities in connection with space manufacturing of reinforced foam composites.

f. Containerless casting of spheres in orbit.

g. Non-contact material handling in orbit.

SECTION 7

FLIGHT EXPERIMENT EVALUATION

The flight experiments were carried out on Apollo 14 by astronaut Roosa during the return flight from the moon on 7 February 1971. Identical control specimens were subjected to the flight processing procedure on the ground by MSFC-S&E-PT. All samples were removed from the capsules by MSFC and cut in half in the longitudinal direction. One half of each flight and control sample No. 5 and No. 11 were turned over to Convair Aerospace on 16 April 1971 for evaluation; the remaining half-samples were retained at MSFC for further reference.

The evaluation procedures and results of Samples 5 and 11 are described in the following sections. The evaluation was carried out in accordance with the procedures outlined in MSFC memo S&E-PT-A (205-453-1664) of 29 March 1971. Emphasis was placed on the investigation of the significant characteristics and phenomena. Procedures are presented in topical outline form, as they have been documented in detail in the Preliminary Evaluation Plan submitted by Convair Aerospace on 1 February 1971.

7.1 DEFINITION AND OBJECTIVES OF SAMPLES 5 AND 11

The primary objective of specimens 5 and 11 was to demonstrate the feasibility of producing high-performance structural materials by dispersion of reinforcements in a molten matrix under zero-g conditions; it utilizes the zero-g phenomenon of mixture stability, not attainable on earth. The composition, processing parameters, and specific objectives of the two samples were as follows:

a. Sample 5

Capsule content: 75% metal, 25% vacuum

Metal composition: In-Bi alloy (66/34) matrix with 6% Cu-Be fibers, 5 mil diam x 100 mil long, coated for perfect wetting characteristics.

Processing: (1) Melting of matrix, (2) shaking of capsule to disperse fibers, and (3) solidification.

Objectives: (1) To demonstrate the uniform dispersion of fibers in the flight sample (liquid-state mixture stability - absence of g-induced segregation); (2) to identify any unpredictable physical or metallurgical effects; and (3) to obtain information on significant processing parameters.

b. Sample 11

Capsule content: 75% paraffin - matrix composite, 25% argon gas at (undetermined) reduced pressure (leakage during EB welding).

Material composition: Paraffin matrix with 6% coated Cu-Be fibers, 5 mil, diam x 100 mil long.

Processing: (1) Melting of matrix, (2) shaking of capsule to disperse fibers, and (3) solidification.

Objectives: (1) To demonstrate the stable dispersion of fibers and gas bubbles (liquid-state mixture stability - absence of g-induced segregation), and (2) to investigate gas bubble-fiber interaction.

7.2 EVALUATION OF SAMPLE 5

The individual evaluations and measurements are presented in the form of a topical outline, with a minimum of data for the purpose of record. Otherwise, the results of individual evaluations and the pertinent documentation are integrated in the interpretation of results in Section 7.3 and the conclusions in Section 7.6.

The flight and control (ground) samples were designated by MSFC as 5F-B and 5C-A, respectively. Additional digits for sections of these samples are identified in Figure 7-1.

7.2.1 EVALUATIONS PRIOR TO SECTIONING

a. Dimensions

b. Weight and bulk density

c. Axial center of gravity

d. Macrophotographs of longitudinal cut surface

e. Spot microphotos of outer surface

f. Definition and interpretation of differences between F and C samples

g. Interpretation of free-end configuration of F sample as example of "free casting."

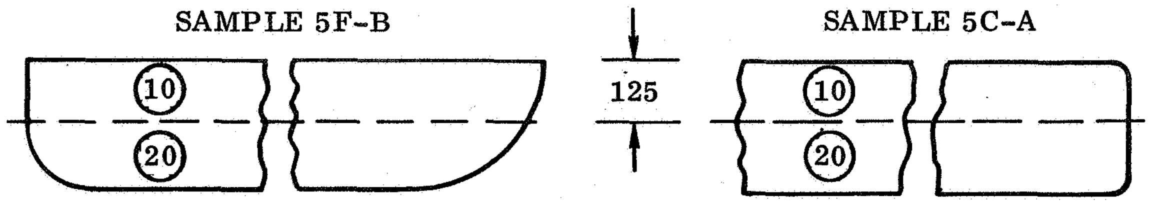

CUT A: HALF-SAMPLE (B, A) CUT LENGTHWISE INTO SECTIONS 10 & 20

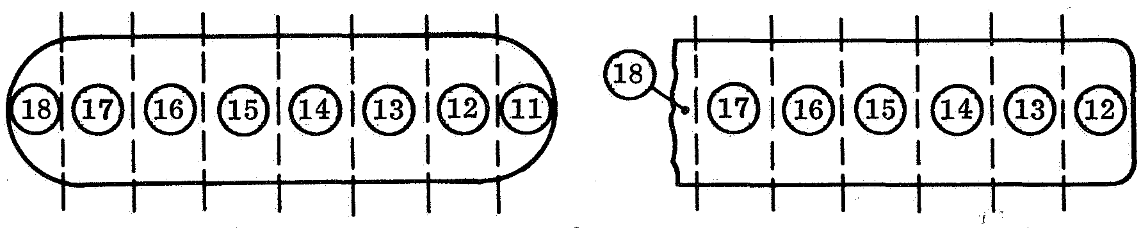

CUT B: SECTIONS 10 CUT RADIALLY INTO SECTIONS 11 THRU 18.
NET WIDTH OF SECTIONS 12 THRU 17 = 300 MILS

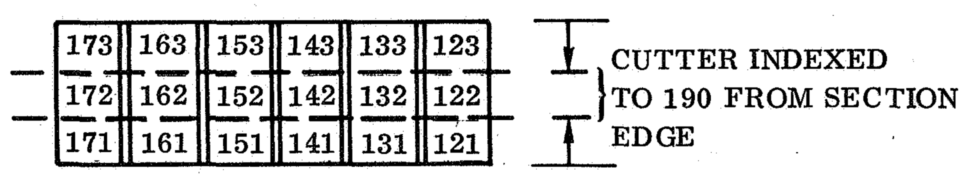

CUT C: SECTIONS 12 THRU 17 CUT INTO 3 PIECES OF EQUAL WIDTH

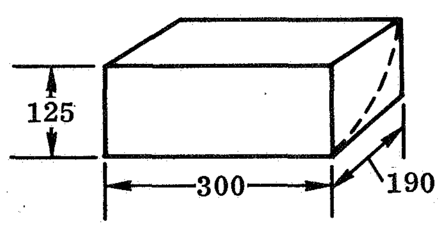

DIMENSIONS OF EACH SPECIMEN (121 THRU 173)

NOTE: ALL DIMENSIONS IN MILS. SKETCHES ON ARBITRARY SCALE.

Figure 7-1. Sectioning Plan - Sample 5

The sample dimensions were measured as follows (in inches):

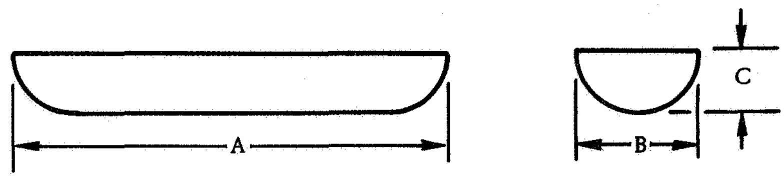

Sample	A	B	C
5F	2.370	0.685	0.310
5C	2.155	0.685	0.320

Weight and bulk density at 23°C were:

	Weight (gm)
5F	45.2650
5C	47.3426

	Bulk Density (gm/cm^3)
5F	8.005
5C	8.053

In view of the irregular sample shape, the measurement of c.g. was inconclusive as to fiber or void distribution.

7.2.2 SECTIONING - SAMPLES 5F-B AND 5C-A

a. Cut A: Sections 10 and 20 (2 pieces)

b. Cut B: Sections 11 through 18 (8 pieces)

c. Cut C: Sections 121 through 173 (18 pieces)

Cuts A, B, C and the pertinent sections are identified in Figure 7-1. Cut A was carried out in a milling machine, using a 30 mil circular mill saw blade (cut width 30 mil nominal, 35 mil maximum). Cuts B and C were carried out with a diamond wire saw (cut width 8 mils).

7.2.3 EVALUATION OF SECTIONS 5F-B-10 AND 5C-A-10 (CUT A)

a. Dimensions, weight, bulk density.

b. Surface photos

c. Neutron radiographs

d. First-order dispersion mapping by surface wire count

e. First-order classification of fiber orientation

f. Interpretation of results

7.2.4 EVALUATION OF SECTIONS 11 AND 18 (CUT B)

a. Micro-effects of surface tension, wetting and apparent mixing characteristics upon surface micro configuration and fiber arrangement

b. Microphotography of significant details

c. Interpretation of results as to potential and problems of metal-metal composite casting

7.2.5 EVALUATION OF SECTIONS 121 THROUGH 173 (CUT C)

a. Metallographic analysis of Sections 142 and 161

b. Weight and bulk density of each of the remaining 16 sections

c. Accurate determination of the wire content of each of the remaining 16 sections by chemical analysis

d. Mapping of fiber dispersion over sample cross section

e. Comparison and interpretation of dispersion differences between F and C samples

The methods of chemical analysis and dispersion mapping were described in the evaluation plan of 1 February 1971, para. 5A.2.1.4 and 5A.2.1.5 (Page 9). The data on weight, bulk density, and chemical composition of the 16 sections 121-141, 143-153 and 162-173 are presented in Table 7-1.

7.2.6 EVALUATION OF SECTION 5F-B-20

Section 20 of the flight sample (only) was cut radially into three sections (21, 22, and 23) for further metallographic analysis of the radial cross-section, particularly for the investigation of a void close to the surface in Section 22.

Table 7-1. Fiber Content and Bulk Densities of Sections 121-173

Note: Fiber content is determined by copper content.

	5C		5F	
Section No.	Cu Content %	Bulk Density (gm/cm^3)	Cu Content %	Bulk Density (gm/cm^3)
121	4.72	8.75	17.82	7.61
122	4.66	8.07	5.98	7.99
123	4.93	8.01	11.34	8.05
131	3.26	8.07	9.54	7.96
132	6.36	8.02	12.64	8.04
133	3.18	8.03	10.30	8.06
141	4.25	8.05	5.83	8.03
142	Metallographic specimen			
143	7.24	7.81	7.29	8.03
151	8.63	7.95	2.86	8.03
152	10.51	7.78	3.43	8.06
153	6.63	7.96	2.50	8.06
161	Metallographic specimen			
162	7.67	8.06	0.01	8.03
163	4.92	8.06	0.78	8.06
171	7.90	8.03	2.77	8.05
172	6.52	7.75	1.09	8.04
173	6.25	8.05	0.81	8.06

7.3 RESULTS - SAMPLE 5

7.3.1 SAMPLE CONFIGURATION. Since the sample occupied only 75% of the capsule volume, it was allowed to move freely after melting within the capsule. The sample configuration after solidification was, therefore, determined by the presence or absence of g, as evidenced by the radiographs of Figure 7-2. While the ground sample (C) which was placed in vertical position for solidification, settled as expected, the configuration of the flight sample (F) was determined by surface tension. The free end displays the spherical shape typical of "free casting." Since the In-Bi alloy did not wet the aluminum capsule, even the cylindrical surface shows only partial contact with the capsule wall and remained essentially "free," as evidenced by comparison of the cylindrical surfaces of the ground and flight samples in Figure 7-3.

7.3.2 FIBER DISPERSION. The dispersion attainable in zero-g was determined by the difference between the flight and ground samples. It was measured by three methods: (1) qualitative visual, (2) fiber count, and (3) chemical analysis.

The qualitative visual difference of dispersion between zero-g and g is illustrated in the polished lengthwise cross-section, Figure 7-4, and the neutron radiograph of a lengthwise slice of 1/8 inch thickness, Figure 7-5. The g-induced segregation of the ground sample (Figures 7-4C and 7-5C) is evident; even though the density difference between fibers and matrix was only 1%, the bulk of the fibers settled in

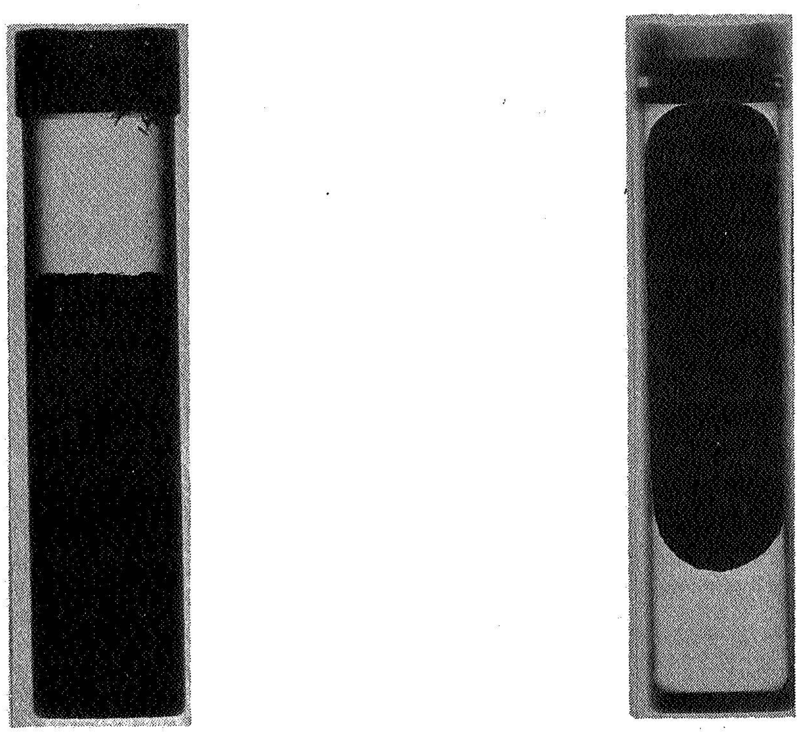

C F

Figure 7-2. Position and Configuration of Samples 5C and 5F in Capsule (Radiographed by MSFC Prior to Capsule Opening)

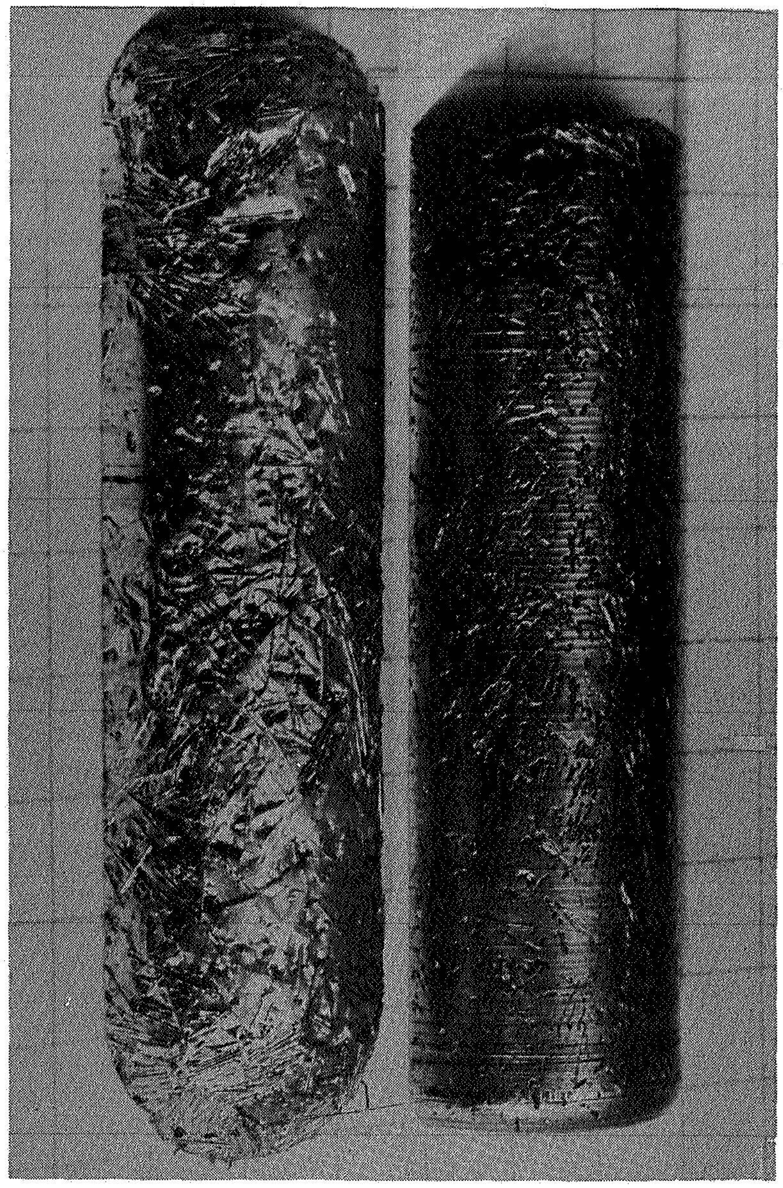

F C

Figure 7-3. Surface of Samples 5F and 5C

the lower section, while the upper section was virtually free of fibers. A smaller amount of fibers was carried up to the top by rising bubbles and surface tension effects (see Section 7.3.4). In the flight sample (Figures 7-4F and 7-5F, the fibers are dispersed over the entire cross-section. Disuniformities of dispersion are the result of the rather primitive mixing method. The patterns in the neutron radiograph (Figure 7-5) indicate that the mixing motion never came to rest and that groups of fibers arranged themselves with the currents of the liquid matrix.

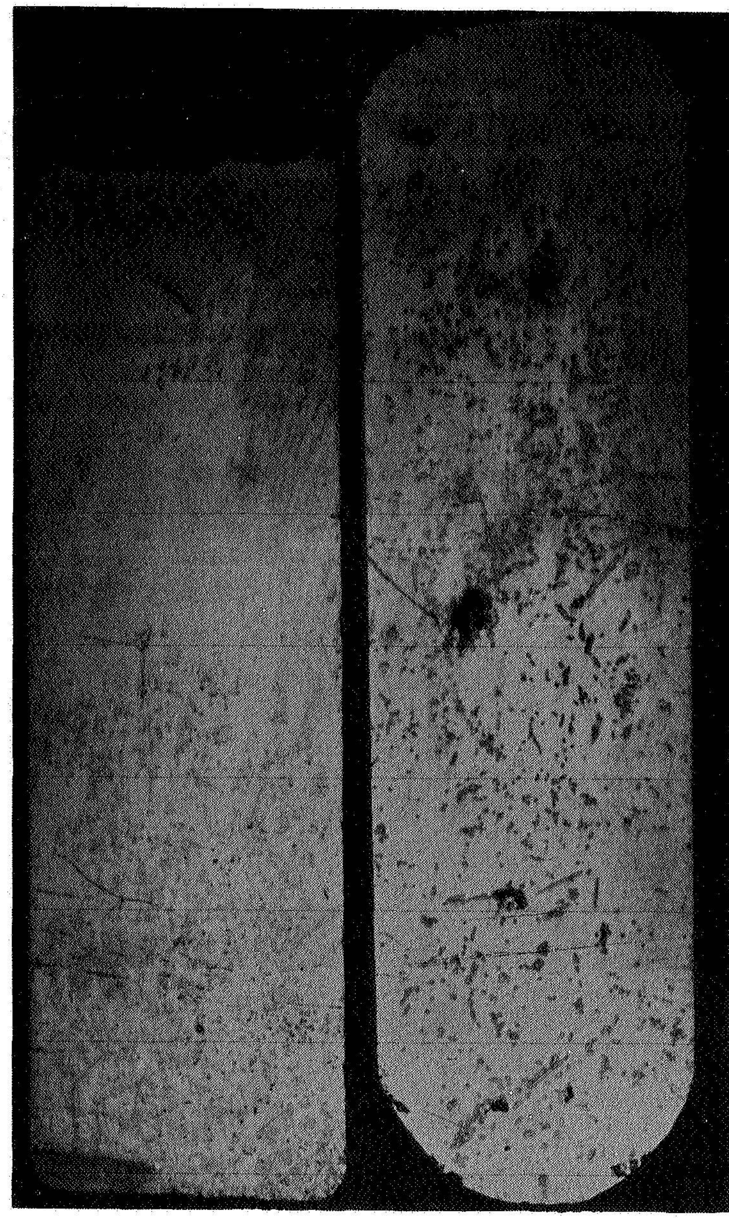

Figure 7-4. Longitudinal Cross-Section of Samples 5C and 5F

The difference in dispersion is more drastically demonstrated by the results of the fiber count over the lengthwise cross-section, which is plotted versus the longitudinal axis in Figure 7-6.

For an accurate measurement of dispersion, a lengthwise 1/8-inch slice of both samples was cut into 18 small specimens, and the fiber content of 16 specimens determined by wet chemical analysis. The results are illustrated in Figure 7-7 by the degree of shading of each section; the numbers in each section identify the bulk densities, or the presence of voids.

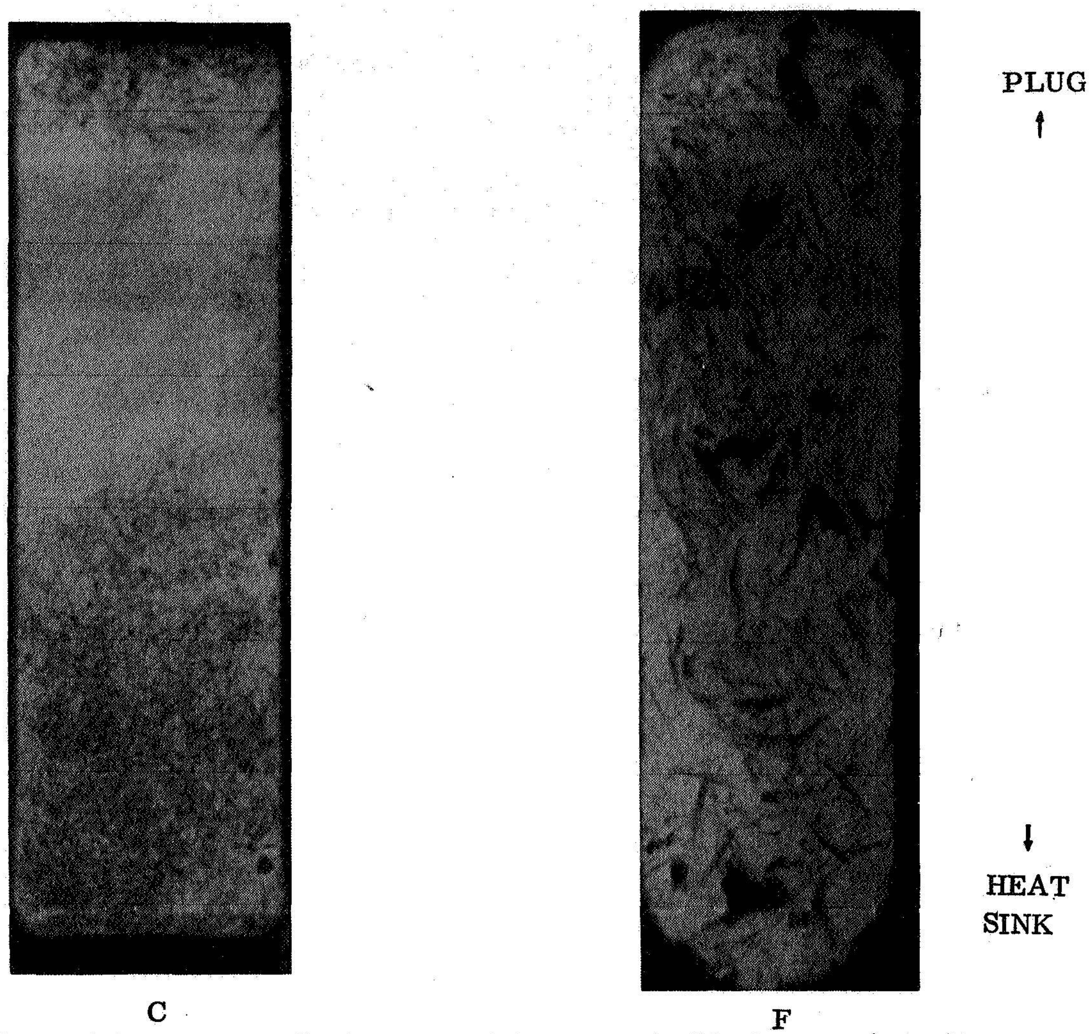

Figure 7-5. Neutron Radiograph of Sections 10 (Thickness 1/8 Inch)

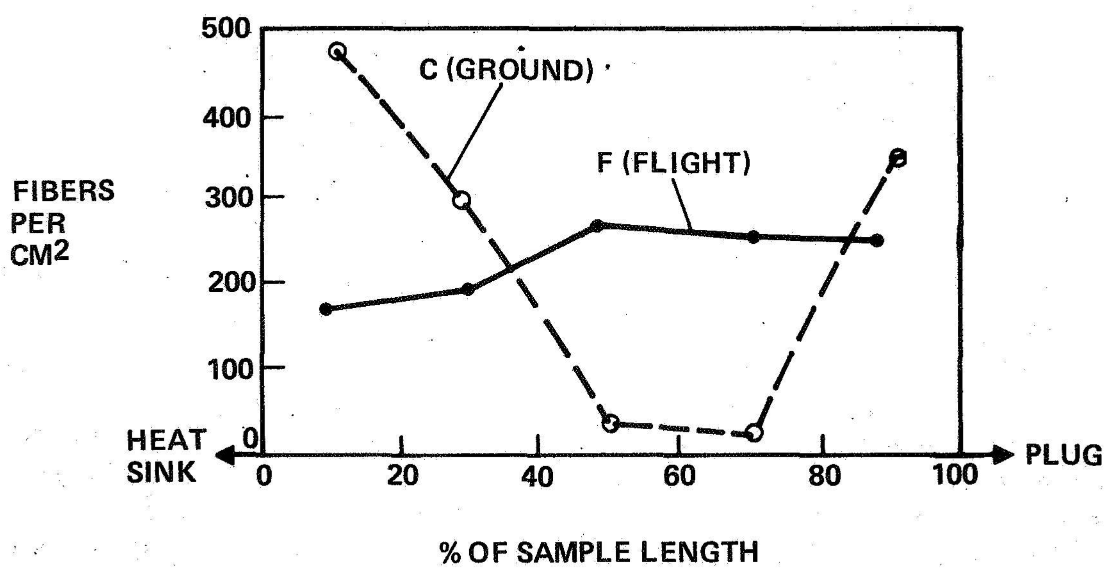

Figure 7-6. Dispersion of Cu-Be Fibers, Determined by Surface-fiber Count (Section 10)

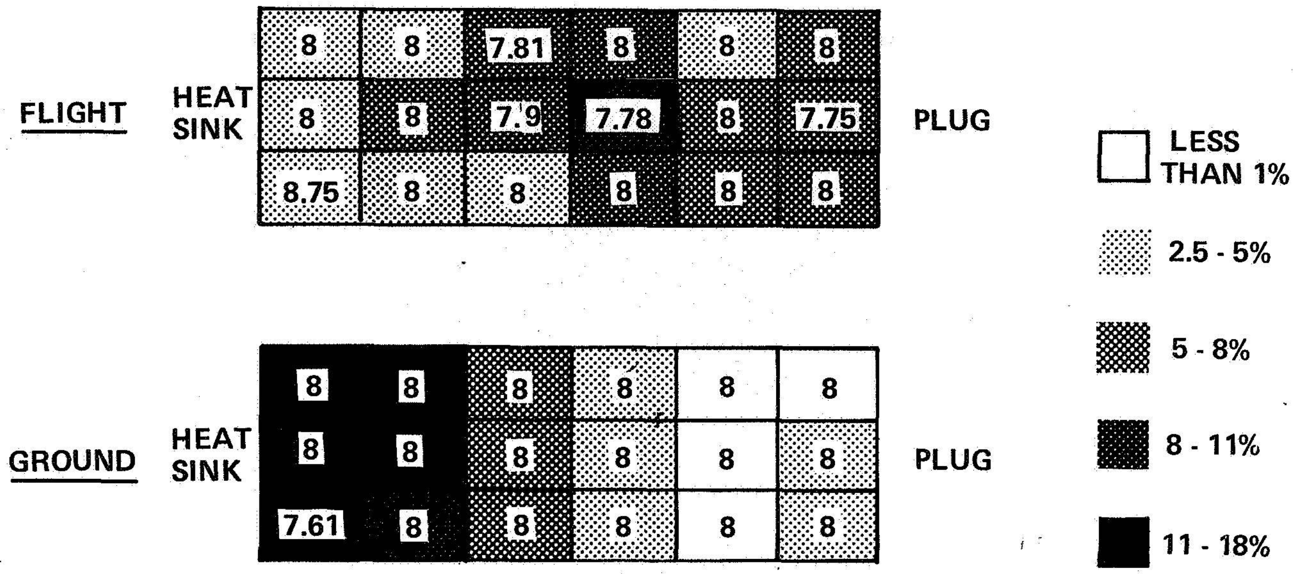

Figure 7-7. Dispersion Map, Established from Chemical Analysis of Sections 111 to 173. Shading Indicates Fiber Content. Numbers Denote Bulk Densities

7.3.3 FIBER ORIENTATION. An examination of surfaces (Figures 7-3 and 7-8) shows that an undisputable tendency of fiber self-alignment present in the flight samples is not present in the ground sample. It is particularly pronounced in the free-cast end of the flight sample (Figure 7-8A). Whether this effect occurs also in the bulk material remains unresolved because prohibitive evaluation difficulties were encountered in this particular matrix material.

This phenomenon could be explained (1) by dipole effects of the fibers, in which case it would also apply to the bulk, (2) by surface tension effects which may also apply to the bulk, (3) by surface tension-liquid/gas interface effects, which would only apply to surfaces, voids or gas bubbles (foam; see Section 7.3.4), or (4) by a combination of these effects.

Regardless of the explanation, if this is a bulk material effect it has considerable applications potential, such as control of preferred fiber orientation by appropriate vibration modes or other means.

7.3.4 FIBER COAGULATION AT INTERFACES. The flight sample has a number of internal voids, resulting from cavitation effects of the mixing process. As evidenced in a larger void, Figure 7-9 and a small void, Figure 7-10, fibers coagulate at the void surface. Since there is no other explanation, this has to be regarded as a true interface effect with a considerable applications potential.

Applied to foams, it would provide a desirable framework of fibers at the surface of each foam cell. Laboratory work has shown that the generation of metal foams

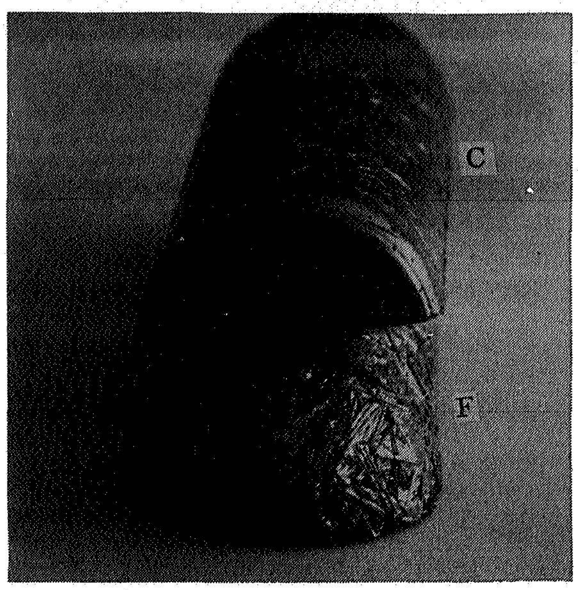

A. Heat-Sink Ends (5C = Bottom;
5F = Face End)

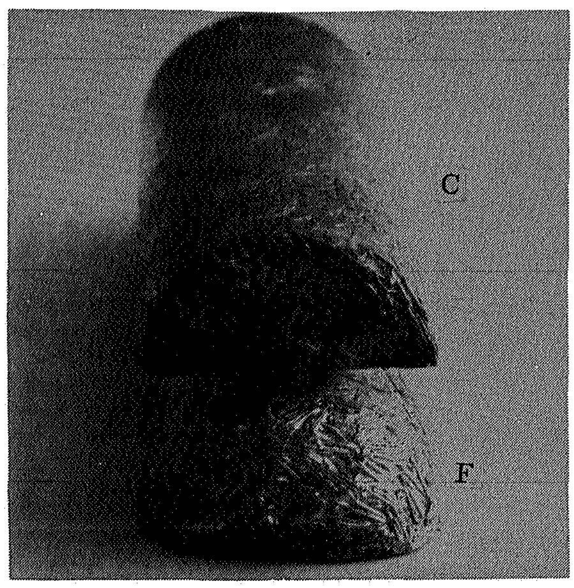

B. Plug-Ends (5C = Top;
5F = Touching Plug)

Figure 7-8. End Surface of Samples 5C and 5F

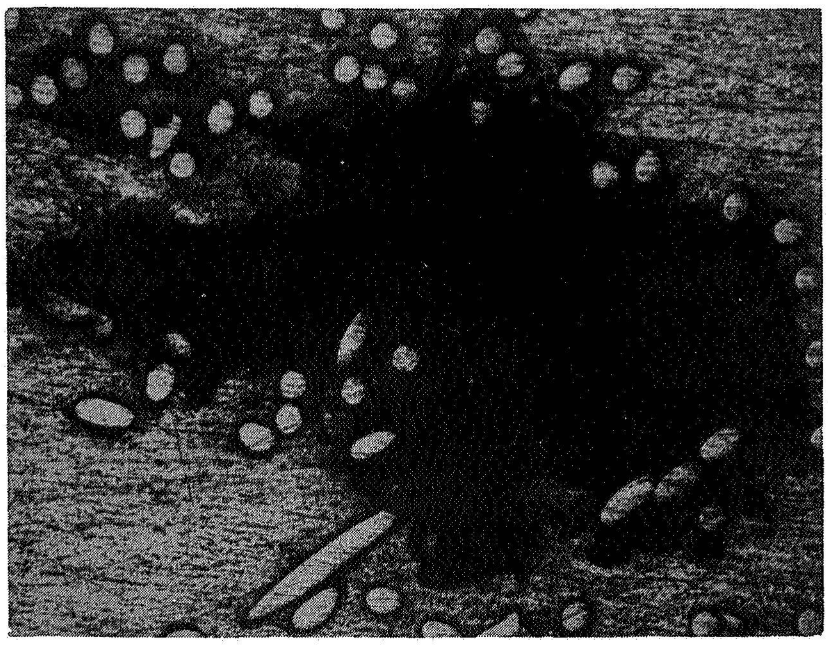

Figure 7-9. Fiber Agglomeration at Large Void (Fiber Diameter = 5 Mil)

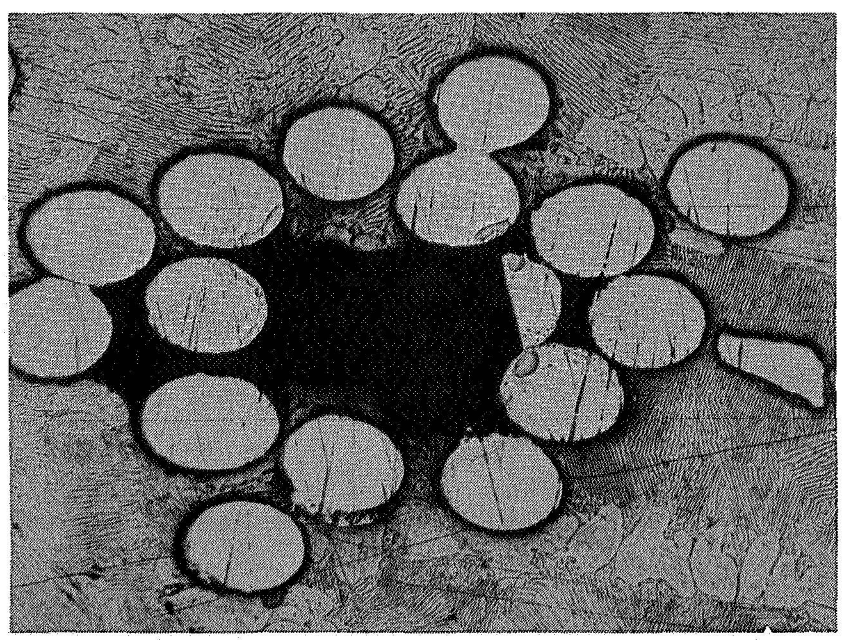

Figure 7-10. Fiber Agglomeration at Small Void (Fiber Diameter = 5 Mil)

requires surface stabilization by the use of an appropriate gas for a specific material. In most cases one will use an oxygen-enriched gas, which stabilizes the surface by generation of an oxide film. This film, in turn, is non-wetting, while the fibers, by postulation, are wetting. This situation offers the unique potential of exact control of fiber location, achievable by an optimum balance between the fiber-rejecting effects of the non-wetting surface, and the fiber attraction to the interface, as observed in this experiment.

The tendency of the fibers to adhere to interfaces also explains the presence of fibers in the top section of the ground sample (Figures 7-4, 7-5 and 7-8); during sample processing, voids or bubbles were generated in the bulk by cavitation which, in turn, attracted fibers from the surrounding material. Upon stop of mixing motion, the buoyancy caused these voids or bubbles to rise to the top, carrying the adhering fibers along.

7.3.5 FORMATION OF SURFACE POCKETS. Microscopic examination of the flight sample surface revealed a number of pockets, as shown in Figure 7-11. Their surface geometry is determined by a frame of several (mostly four) fibers. They extend quite deep into the bulk (1/8 inch) and exhibit straight walls, retaining the surface geometry. These pockets cannot be explained by surface tension, which would postulate a rather shallow, curved pocket. With the present limitations of analysis and experimental evidence, this phenomenon remains unexplained.

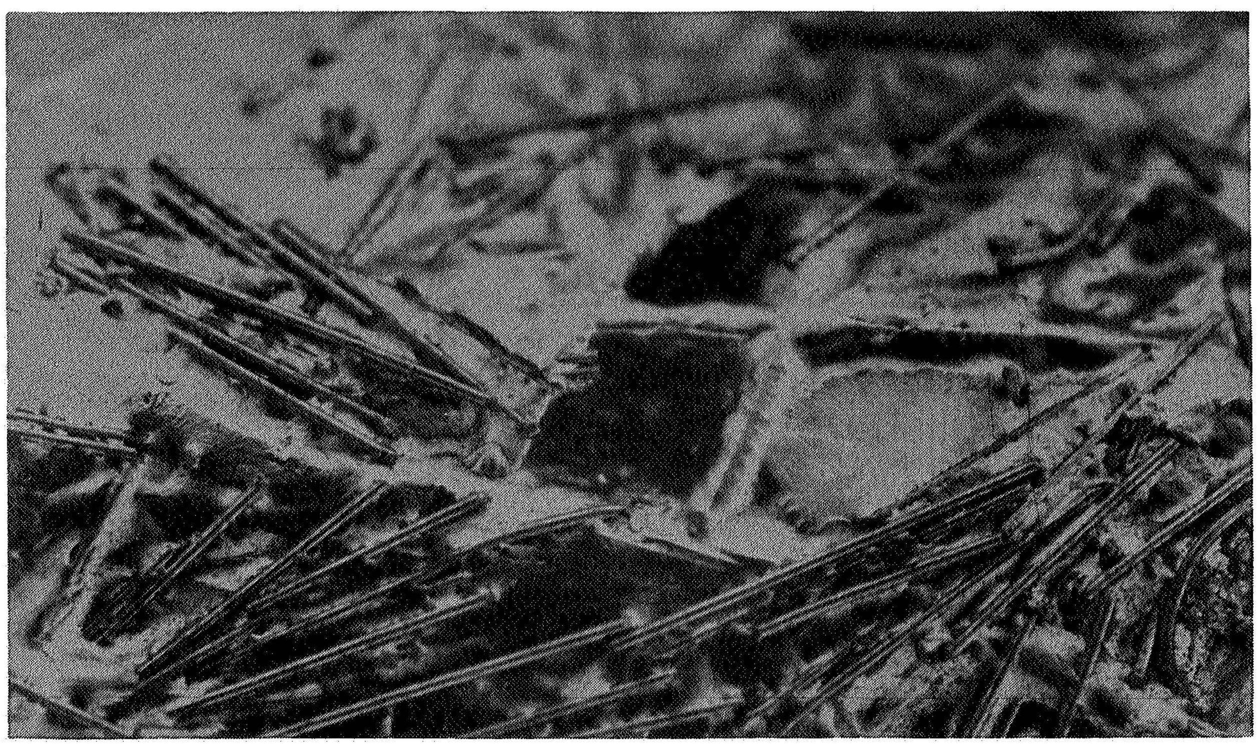

Figure 7-11. Typical Surface Pocket Formation in Flight Sample

7.3.6 METALLURGICAL EFFECTS. In this, as well as in other samples, a pronounced formation of dendrites was observed in the flight sample; they were not present in the ground sample. The dendrites are shown in Figure 7-12 and in the micrograph, Figure 7-13B. The ground sample microstructure is represented in Figure 7-13A. The cooling profile was identical in both the flight and ground samples; there are three potential explanations: (1) formation of dendrites is a zero-g effect, (2) the fibers act as nulceation sites for the formation of dendrites, as can be observed at several places in Figure 7-12 (since this is an arbitrary plane, some dendrites may originate at fibers below the visible surface) and (3) there was a difference in matrix composition between ground and flight sample (unlikely).

7.4 EVALUATION OF SAMPLE 11

As for Sample 11, the evaluation procedure is presented in form of a topical outline, while the results are integrated in the discussion of results in Section 7.5 and the conclusions, Section 7.6.

The flight and control samples were designated by MSFC as 11F-A and 11C-A, respectively. Additional digits for sections of these samples are identified in Figure 7-14.

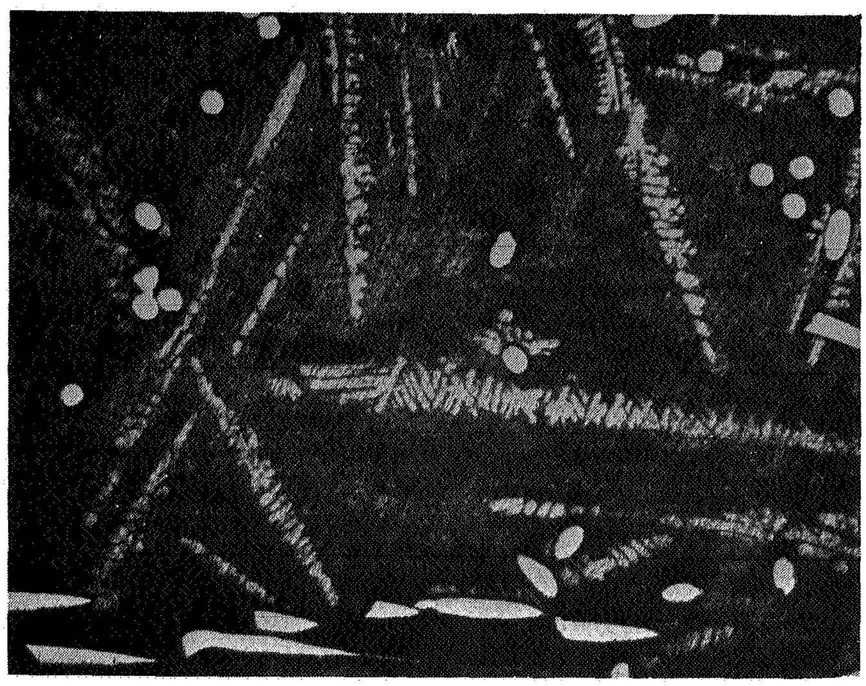

Figure 7-12. Dendrites in Sample 5F. (Note Start of Dendrite Formation at Fiber in Center.)

A. Sample 5C — 100% Eutectic

B. Sample 5F — Dendrites + Eutectic

Figure 7-13. Microstructures of Samples 5C and 5F

CUT A:

HALF-SAMPLES
CUT LENGTHWISE
INTO SECTIONS
10 & 20

CUTS B:

SECTION 20 CUT
INTO 3 PIECES
IDENTIFIED AS
SECTIONS 21, 22, 23

CUTS C:

EACH SECTION
21, 22, 23 CUT
in HALF
HALVES DESIGNATED
a, b

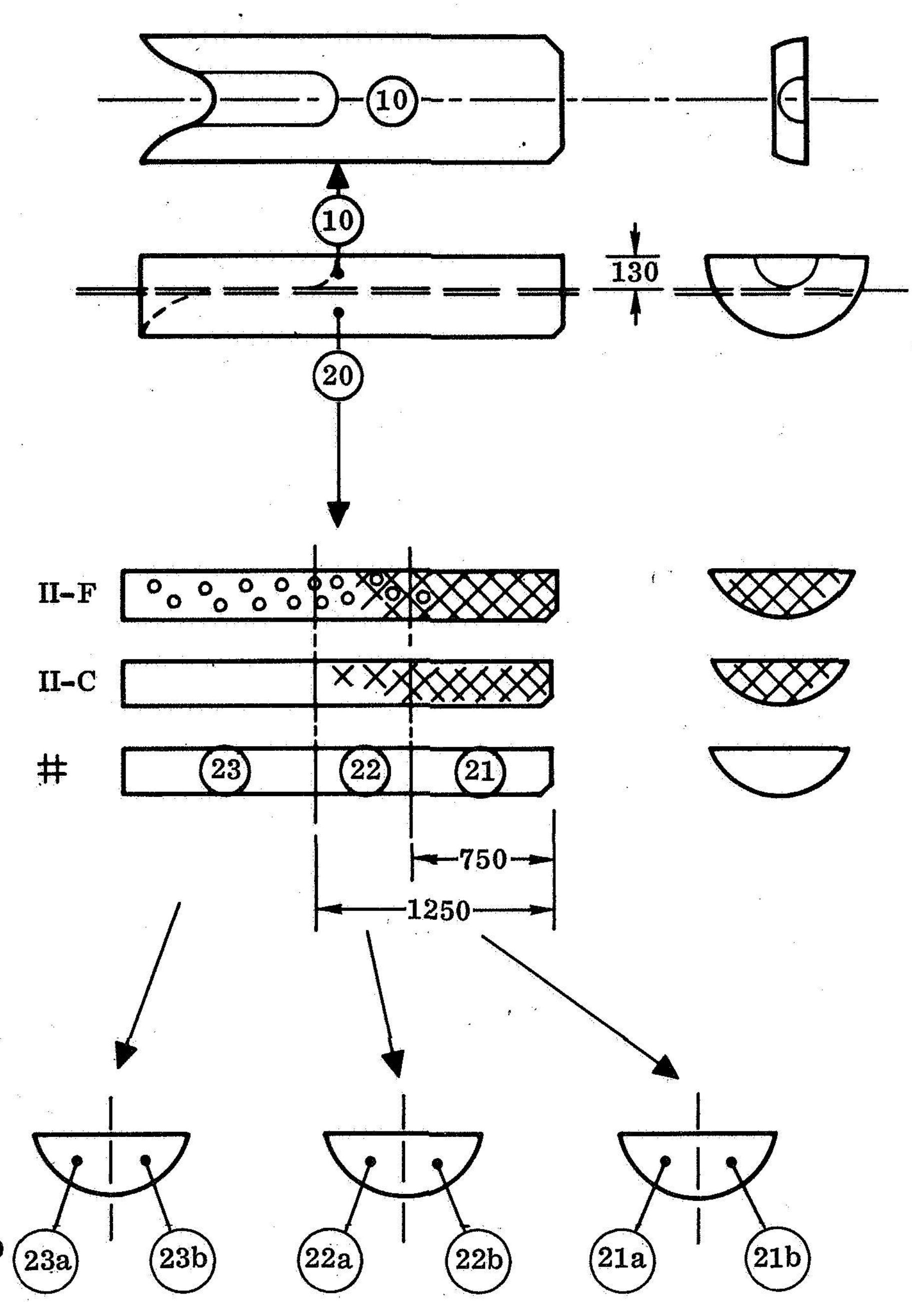

NOTE: ALL DIMENSIONS IN MILS. SKETCHES ON ARBITRARY SCALE

Figure 7-14. Sample 11 Sectioning Plan

7.4.1 EVALUATIONS OF SAMPLES 11F-A AND 11C-A PRIOR TO SECTIONING

a. Dimensions

b. Weight and bulk density

c. X-ray radiographs

d. Macrophotographs

7.4.2 SECTIONING - SAMPLES 11F-A AND 11C-A

a. Cut A: Sections 10 and 20 (two pieces)

b. Cut B: Sections 21, 22, 23 (three pieces)

c. Cut C: Sections 21A through 23B (six pieces)

Cuts and sections are identified in Figure 7-14. All cuts were carried out by a diamond wire saw with a cut width of 8 mils.

7.4.3 EVALUATION OF SECTIONS 11F-A-10 AND 11C-A-10 (CUT A)

a. Interpretation of F and C shrinkage void configuration.

b. Microscopic investigation of bubbles in the pure paraffin section and in the paraffin-fiber interphase zone.

c. Macrophotographs.

d. Definition and interpretation of differences between F and C samples.

7.4.4 EVALUATION OF SECTIONS 21 THROUGH 23 (CUT B)

a. Investigation of bubble dispersion (Sections 22, 23).

b. Macrophotos of bubble dispersion (Sections 22, 23).

c. Investigation of fiber agglomeration in Section 21.

7.4.5 EVALUATION OF SECTIONS 21a, 22a AND 23a (CUT C)

a. Melting in vertical glass tube observing behavior of bubbles and gray matter.

b. Spectrographic analysis of gray matter.

7.4.6 SECTIONS 11-F-22b AND 23b. Retained for further reference.

7.5 RESULTS - SAMPLE 11

7.5.1 CONFIGURATION. As evidenced by Figure 7-15, there is practically no difference between the configurations of the ground and flight samples (11C and 11F). This implies that the flight sample was subjected to a g-force after mixing which shifted the entire liquid mass to one capsule end. It is, however, likewise evident

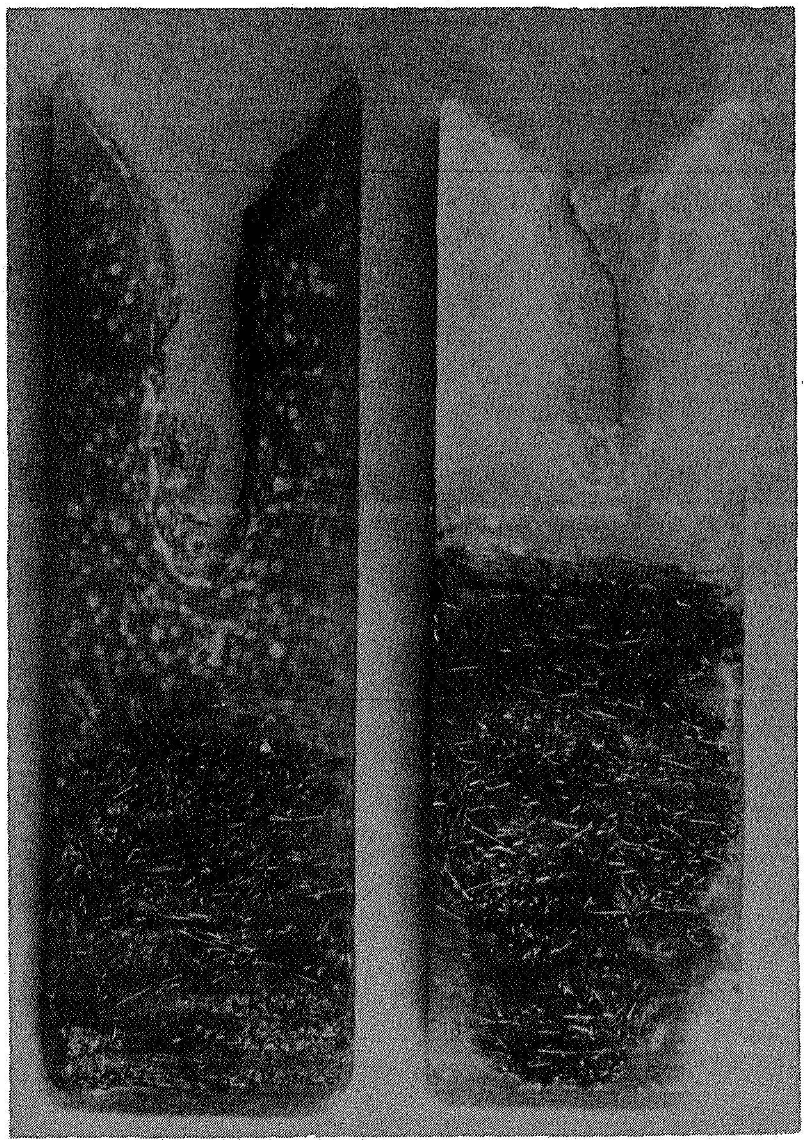

PLUG ↑

↓ HEAT SINK

11F 11C

Figure 7-15. Longitudinal Cross-Section of Samples 11F and 11C that this g-force was only transient and no longer in existence during cooling since there is no segregation of gas bubbles. These bubbles were very likely formed during cooling of the liquid paraffin prior to solidification.

The configuration exhibits a large shrinkage void, which was to be expected. The sample dimensions were measured as follows (in inches):

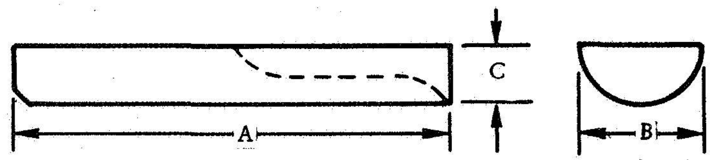

Sample	A	B	C
11F	2.280	0.685	0.365
11C	2.175	0.695	0.355

Due to the concentration of the fibers at one end, discussed below, there was no reason for measuring bulk densities or the center of gravity.

7.5.2 FIBER DISPERSION. At the time of sample preparation, only coated fibers were available for the flight sample, 11F. Since the processing temperature was higher than the melting temperature of the coating, the coating melted during processing, causing the fibers to literally solder themselves into one single block of paraffin-fiber composite, while the remaining part of the sample was pure paraffin (Figure 7-15). Consequently, the objectives of fiber dispersion and fiber-bubble interaction were not achieved.

7.5.3 BUBBLE DISPERSION. As can be observed by comparison of the flight sample (Figure 7-15-11F) and the ground sample (Figure 7-15-11C), a stable dispersion of gas bubbles has been achieved under zero-g conditions, while all bubbles in the ground sample were removed by buoyancy. The close-up of the bubbles is shown in Figure 7-16. A black coloring of the bubbles at the surface, resulting from sample cutting, was deliberately retained to distinguish them from the bubbles below the surface (light). In view of the limited amount of gas present, only a low bubble density was obtained, eliminating the problems of bubble coalescence and surface stabilization.

The bubble gas may also have originated from volatiles of the paraffin. However, for the objective of this experiment, the source of the gas is immaterial.

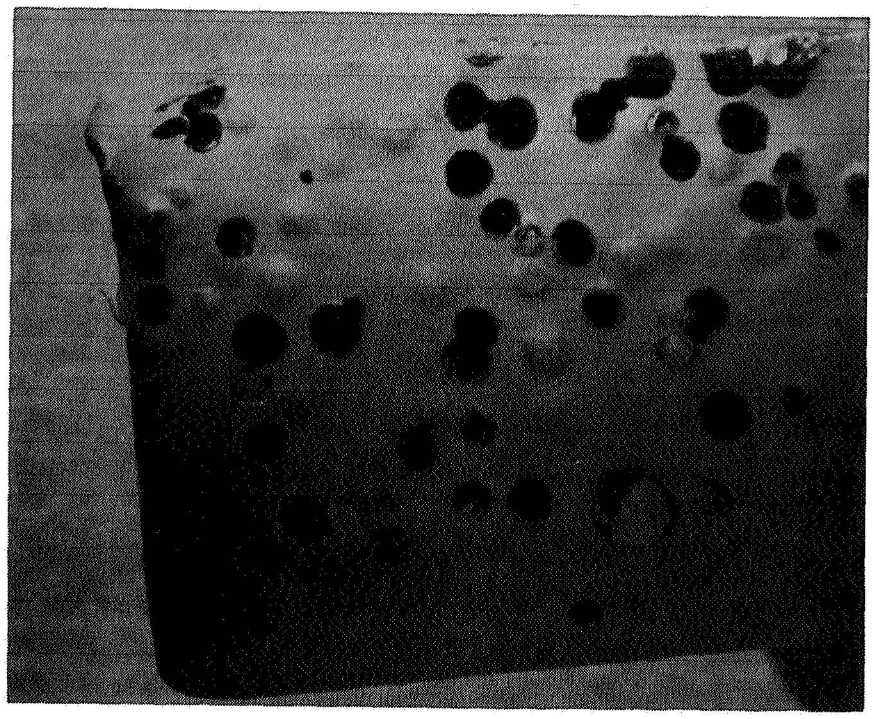

Figure 7-16. Close-up of Bubble Dispersion in Flight Sample 11F
(Bubbles in cut-surface distinguished by dark coloring)

7.6 CONCLUSIONS - SAMPLES 5 AND 11

The significant results of experiments 5 and 11 may be summarized as follows:

a. A uniform and stable dispersion of fibers in a molten metal can be obtained under zero-g conditions. This proves the feasibility of providing high-performance composite materials and cast components, which are not attainable in the one-g environment.

b. The tendency of fiber coagulation at gas interfaces greatly enhances the feasibility of producing fiber-reinforced foams for use as materials or cast components with highest stiffness and strength-to-weight ratio.

c. The not-yet-conclusive tendency of fiber alignment offers the potential of producing high-performance composite materials and components with controlled fiber orientation.

d. The stability of bubbles in a liquid matrix is demonstrated. It represents the basis for the development of plain and reinforced metal foams, feasible only under zero-g conditions.

e. The generation of foams requires considerable process development efforts. It cannot be expected that useful foams will be obtained merely by shaking (cavitation). Developmental efforts are further indicated in interface (surface) stabilization with gases and in mixing techniques for fiber dispersion.